Molecular Neurobiology (2019) 56:935–953
https://doi.org/10.1007/s12035-018-1126-5

Early Downregulation of p75^{NTR} by Genetic and Pharmacological Approaches Delays the Onset of Motor Deficits and Striatal Dysfunction in Huntington's Disease Mice

Nuria Suelves[1,2,3] · Andrés Miguez[1,2,3] · Saray López-Benito[4,5] · Gerardo García-Díaz Barriga[1,2,3] · Albert Giralt[1,2,3] · Elena Alvarez-Periel[1,2,3] · Juan Carlos Arévalo[4,5] · Jordi Alberch[1,2,3] · Silvia Ginés[1,2,3] · Verónica Brito[1,2,3]

Received: 13 March 2018 / Accepted: 11 May 2018 / Published online: 27 May 2018

Abstract

Deficits in striatal brain-derived neurotrophic factor (BDNF) delivery and/or BDNF/tropomyosin receptor kinase B (TrkB) signaling may contribute to neurotrophic support reduction and selective early degeneration of striatal medium spiny neurons in Huntington's disease (HD). Furthermore, we and others have demonstrated that TrkB/p75^{NTR} imbalance in vitro increases the vulnerability of striatal neurons to excitotoxic insults and induces corticostriatal synaptic alterations. We have now expanded these studies by analyzing the consequences of BDNF/TrkB/p75^{NTR} imbalance in the onset of motor behavior and striatal neuropathology in HD mice. Our findings demonstrate for the first time that the onset of motor coordination abnormalities, in a full-length knock-in HD mouse model (KI), correlates with the reduction of BDNF and TrkB levels, along with an increase in p75^{NTR} expression. Genetic normalization of p75^{NTR} expression in KI mutant mice delayed the onset of motor deficits and striatal neuropathology, as shown by restored levels of striatal-enriched proteins and dendritic spine density and reduced huntingtin aggregation. We found that the BDNF/TrkB/p75^{NTR} imbalance led to abnormal BDNF signaling, manifested as a diminished activation of TrkB-phospholipase C-gamma pathway but upregulation of c-Jun kinase pathway. Moreover, we confirmed the contribution of the proper balance of BDNF/TrkB/p75^{NTR} on HD pathology by a pharmacological approach using fingolimod. We observed that chronic infusion of fingolimod normalizes p75^{NTR} levels, which is likely to improve motor coordination and striatal neuropathology in HD transgenic mice. We conclude that downregulation of p75^{NTR} expression can delay disease progression suggesting that therapeutic approaches aimed to restore the balance between BDNF, TrkB, and p75^{NTR} could be promising to prevent motor deficits in HD.

Keywords Huntington's disease · p75^{NTR} · TrkB · BDNF · Motor deficits onset · Striatal pathology

Introduction

Huntington's disease (HD) is a fatal neurodegenerative disorder with a characteristic phenotype including chorea and dystonia, incoordination, cognitive decline, and psychiatric symptoms [1]. It is caused by an abnormal expansion of a CAG codon in exon 1 of the *huntingtin* gene [2]. Neuropathological hallmarks include intranuclear aggregates of mutant huntingtin and selective neurodegeneration of striatal medium spiny neurons (MSNs) [3, 4], which are the principal projection neurons within the striatum. Survival and maintenance of MSNs are especially dependent on the brain-derived neurotrophic factor (BDNF)-tropomyosin receptor kinase B (TrkB) signaling pathway [5, 6], and the selective vulnerability in HD has been linked to reduced neurotrophic support caused by reduced levels of BDNF [7–10]. Therefore, exogenous

Electronic supplementary material The online version of this article (https://doi.org/10.1007/s12035-018-1126-5) contains supplementary material, which is available to authorized users.

✉ Verónica Brito
veronica.brito@ub.edu

[1] Departament de Biomedicina, Facultat de Medicina, Institut de Neurosciències, Universitat de Barcelona, Barcelona, Spain

[2] Institut d'Investigacions Biomèdiques August Pi i Sunyer (IDIBAPS), Barcelona, Spain

[3] Centro de Investigación Biomédica en Red sobre Enfermedades Neurodegenerativas (CIBERNED), Madrid, Spain

[4] Department of Cell Biology and Pathology, Instituto de Neurociencias de Castilla y León (INCyL), University of Salamanca, Salamanca, Spain

[5] Institute of Biomedical Research of Salamanca (IBSAL), Salamanca, Spain

BDNF administration or pharmacological treatments that raise BDNF levels have been proposed and extensively studied to slow or prevent the HD disease progression. However, these therapeutic strategies only ameliorate or partially improve morphological phenotypes or motor and cognitive behavior in different HD mouse models [11–14]. Several studies suggest that BDNF signaling deficits can be related not only to altered BDNF delivery but also to inappropriate levels of expression or activation of its receptors, TrkB and/or $p75^{NTR}$ [15–21]. TrkB is a member of the neurotrophin tyrosine receptor kinase family that activates cytosolic signaling cascades to promote survival and maintain neurochemical and morphological properties of neurons. On the other hand, BDNF binds also to $p75^{NTR}$, a member of the tumor necrosis factor receptor superfamily [22]. $p75^{NTR}$ can potentiate or reduce Trks signaling, promoting or hampering cell growth and survival depending on the cellular context and Trks or neurotrophins abundance, but it can also act independently activating NF-Kβ, c-Jun kinase (JNK), and RhoA/ROCK pathways [23–25]. $p75^{NTR}$, which is known to be induced in several disease conditions, can activate degenerative pathways, particularly in states in which deficiency of neurotrophins or Trks occurs [26, 27]. Importantly, it has been demonstrated that signaling via either TrkB or $p75^{NTR}$ receptors is compromised in HD. Downregulation of TrkB receptor levels or defects in TrkB signaling have been reported in HD cellular models and HD mice brain [14, 15, 17–21] while increased levels of $p75^{NTR}$ have been demonstrated in the striatum and hippocampus of different HD mouse models [19, 28–30]. These observations support the idea that a correctable defect in the response to BDNF underlies striatal dysfunction in HD. However, no studies have examined the precise contribution of the BDNF/TrkB/$p75^{NTR}$ pathway in the onset of HD motor coordination deficits. Based on these previous reports, we hypothesized that motor behavioral abnormalities in HD are directly associated with improper expression of $p75^{NTR}$, TrkB, and BDNF. Therefore, neuroprotective therapy for HD must involve the reestablishment of not only BDNF but also the complete BDNF/TrkB/$p75^{NTR}$ system. To test our hypothesis, motor behavior and striatal neuropathology were evaluated along the disease progression in double-mutant mice, expressing one copy of mutant huntingtin but heterozygous for $p75^{NTR}$ (KI:$p75^{+/-}$). Our results showed that genetic normalization of $p75^{NTR}$ expression in mutant $Hdh^{Q7/Q111}$ (KI) mice delayed by several months the onset of motor coordination deficits and striatal neuropathology. This improvement might be attributed to the prevention of BDNF/TrkB/$p75^{NTR}$ imbalance, the normalization of BDNF-TrkB-phospholipase C-gamma (PLCγ) signaling, and/or the attenuation of the $p75^{NTR}$-associated JNK pathway. Importantly, at 10 months of age, downregulation of $p75^{NTR}$ is not enough to achieve this improvement supporting the hypothesis that proper levels of TrkB and BDNF are also needed to prevent HD progression. We validated this hypothesis by showing that chronic infusion of fingolimod (FTY720) improved motor coordination behavior and striatal neuropathology in HD transgenic mice which were associated with normalization of $p75^{NTR}$ levels in the BDNF/TrkB/$p75^{NTR}$ system.

Results

Normalization of $p75^{NTR}$ Levels in the Striatum of KI Mice Delays the Onset of Motor Coordination Deficits

We have described that mutant KI mice manifest motor coordination impairments at the age of 8 months [31]. Given the critical role of $p75^{NTR}$ in HD pathology, we evaluated whether normalization of striatal $p75^{NTR}$ levels prevents these motor deficits. To address this question, levels of $p75^{NTR}$ were normalized in KI mice by crossmating of $Hdh^{Q7/Q111}$ with $p75^{NTR}$/Exon $III^{+/-}$ mice ($p75^{+/-}$ mice) to obtain double-mutant mice (KI:$p75^{+/-}$). First, $p75^{NTR}$ levels were analyzed by Western Blot in striatal extracts from wild type (WT), $p75^{+/-}$, KI, and KI:$p75^{+/-}$ mice. As expected, quantification of band intensities revealed a significant increase of $p75^{NTR}$ in KI mice, which was significantly reversed in KI:$p75^{+/-}$ mice at the three different ages evaluated (6, 8, and 10 months) (Fig. 1a). In contrast, no increased expression of $p75^{NTR}$ was observed in the cortex of HD mice according to previous published data by our group [28]. Therefore, both $p75^{+/-}$ and KI:$p75^{+/-}$ mice presented reduced cortical $p75^{NTR}$ levels compared with WT mice (Supplemental Fig. 1A). Next, motor coordination was evaluated. Mice were first trained at 10 rpm during three consecutive days (Fig. 1b), and performance in the rotarod at 10 and 24 rpm was assessed longitudinally in WT, KI, $p75^{+/-}$, and KI:$p75^{+/-}$ mice from 7 to 12 months of age (Fig. 1c). Motor coordination was severely impaired in KI mice starting at 8 months of age and worsening thereafter, with a number of falls significantly higher than WT mice along trials (Fig. 1c). We observed a significant reduction of number of falls in KI:$p75^{+/-}$ mice compared with KI mice at 8 and 9 months when evaluated at 24 rpm while at 10 rpm, these differences were significant only at 9 months. Similar results were obtained when spontaneous locomotor activity was measured in the open field (Fig. 1d). KI mice manifested a significant reduction in the distance traveled compared with WT mice at 8 and 10 month of age while KI:$p75^{+/-}$ mice only displayed significant differences at 10 months of age. At 8 months,

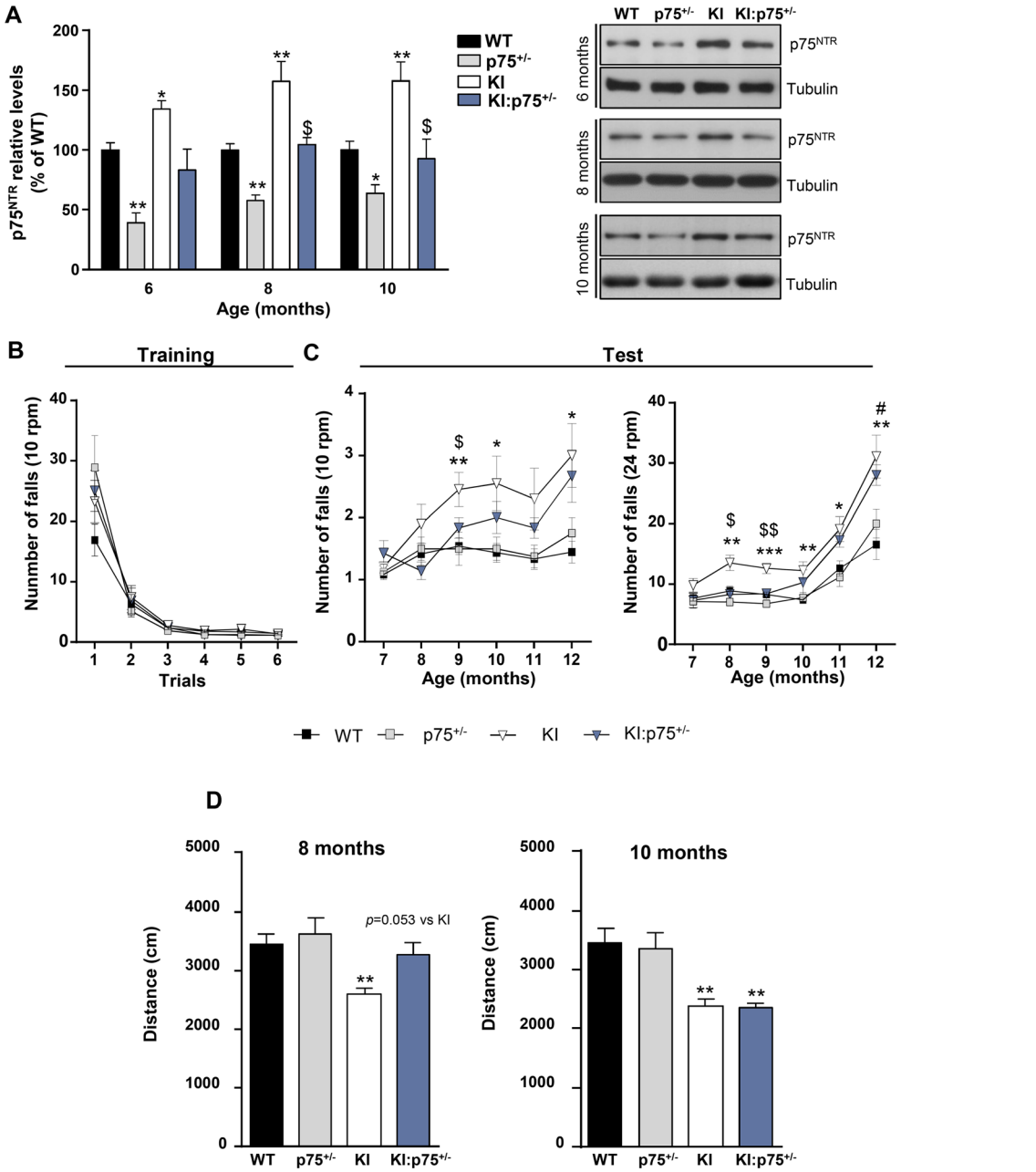

Fig. 1 Normalization of $p75^{NTR}$ expression in KI mice delays the onset of motor deficits. **a** Representative immunoblots showing the levels of $p75^{NTR}$ and tubulin as loading control in striatal extracts obtained from WT, $p75^{+/-}$, KI, and KI:$p75^{+/-}$ mice at 6, 8, and 10 months of age. Histograms represent the relative protein levels expressed as percentage of WT values. All data are shown as the mean ± SEM ($n = 5$–7 mice/genotype/age). Data were analyzed by one-way ANOVA followed by Tukey's test. $^{*}P < 0.05$ and $^{**}P < 0.01$ compared with WT; $^{\$}P < 0.05$ compared with KI. Motor behavior was analyzed in WT, $p75^{+/-}$, KI, and KI:$p75^{+/-}$ by performing the rotarod task (**b**, **c**) and the open field (**d**). **b** The number of falls from a fixed speed rotarod was recorded during 60 s (s) at 10 rpm during training at the age of 5–6 months during three consecutive days. **c** The number of falls from a fixed speed rotarod was recorded during 60 s at 10 rpm and 24 rpm every 4 weeks from 7 to 12 months of age. Data are shown as the mean ± SEM ($n = 10$–13 animals/genotype). At different stages of the disease progression, data were analyzed by one-way ANOVA followed by Tukey's test. $^{*}P < 0.05$, $^{**}P < 0.01$, and $^{***}P < 0.001$: KI compared with WT; $^{\$}P < 0.05$ and $^{\$\$}P < 0.01$: KI:$p75^{+/-}$ compared with KI; $^{\#}P < 0.05$: KI:$p75^{+/-}$ compared with WT. **d** Spontaneous locomotor activity in the open field test at 8 and 10 months of age. Data were analyzed by one-way ANOVA followed by Tukey's test ($n = 10$–13 mice per genotype). $^{**}P < 0.01$ compared with WT

performance in open field by KI:$p75^{+/-}$ mice was comparable to WT mice, traveling more distance than KI mice, although these differences were not statistically significant ($P = 0.053$). Altogether, these data indicate that normalization of striatal $p75^{NTR}$ levels in KI mice delays the onset of motor coordination impairments.

Normalization of p75^{NTR} Levels in the Striatum of KI Mice Delays Striatal Neuropathology

Reduced levels of striatal proteins such as dopamine- and cAMP-regulated phosphoprotein Mr 32 kDa (DARPP32) [32], phosphodiesterase 10A (PDE10A) [33], or adenosine receptor type 2A (A2AR) [34] have been reported in several experimental models of HD and associated with striatal dysfunction. In accordance with these data, a significant decrease in these three proteins was found in KI striatal extracts at 6, 8, and 10 months of age (Fig. 2a–c). Interestingly, in KI:p75$^{+/-}$ mice, the levels of these striatal markers were preserved until 10 months of age, when a similar reduction was observed. Our results support the idea that striatal pathology can be delayed by normalization of p75^{NTR} levels. To further confirm this hypothesis, two other neuropathological hallmarks of HD striatal dysfunction, such as mutant huntingtin (mHtt) aggregates [3, 4] and dendritic spine alterations [35, 36], were analyzed in mice aged between 7 and 10 months. First, mHtt aggregates were detected by EM48 diaminobenzidine staining in the striatum of KI and KI:p75$^{+/-}$ mice (Fig. 3a). A significant reduction in both the number of positive nuclear inclusions and EM48 labeling intensity (staining index) was found in KI:p75$^{+/-}$ compared with KI mice between 8 and 9 months (Fig. 3a), while similar aggregate density and staining index were observed at 10 months in both KI and KI:p75$^{+/-}$ mice (Fig. 3b). Next, DiOlistic labeling was performed to analyze dendritic spine density in fixed brain slices obtained from WT, p75$^{+/-}$, KI, and KI:p75$^{+/-}$ at 7–8 months (Fig. 3c) and 10 months of age (Fig. 3d). The number of spines per micrometer of dendrite length was significantly reduced in KI mice at the different ages evaluated, while a significant increase was observed in KI:p75$^{+/-}$ mice when compared with KI mice. Surprisingly, p75$^{+/-}$ presented a significant increase in spine density when compared with WT mice at 7–8 months, while only an increasing trend at 10 months of age. These results are in accordance with the negative role of p75^{NTR} in dendritic spine density previously reported [37]. Interestingly, at earlier disease stages (3 months), no differences were observed between genotypes supporting the hypothesis that p75^{NTR} downregulation in the striatum prevents the loss of dendritic spines during the course of the disease

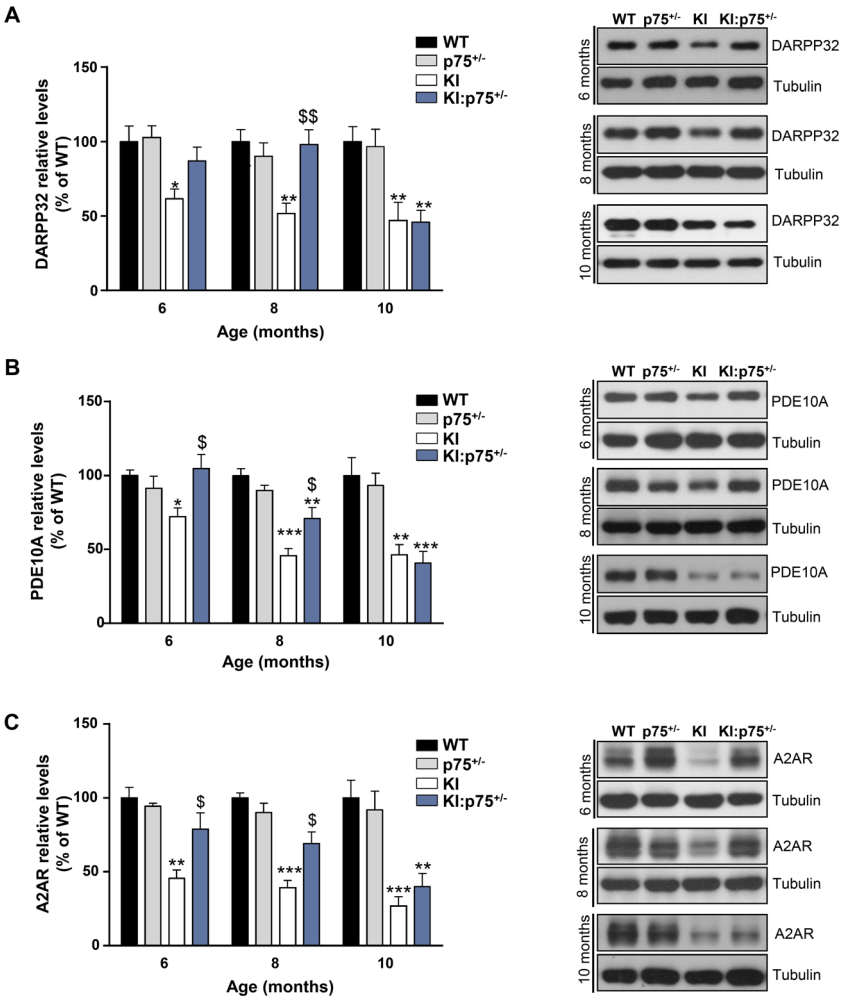

Fig. 2 Normalization of p75^{NTR} expression in KI mice delays the decrease of striatal-enriched proteins. Representative immunoblots showing the levels of DARPP32 (**a**), PDE10A (**b**), A2AR (**c**), and tubulin as loading control in striatal extracts obtained from WT, p75$^{+/-}$, KI, and KI:p75$^{+/-}$ mice at 6, 8, and 10 months of age. Histograms represent the relative protein levels expressed as percentage of WT values. All data are shown as the mean ± SEM ($n = 5$–7 mice/genotype/age). Data were analyzed by one-way ANOVA followed by Tukey's test. *$P < 0.05$, **$P < 0.01$, and ***$P < 0.001$ compared with WT; $^{\$}P < 0.05$ and $^{\$\$}P < 0.01$ compared with KI

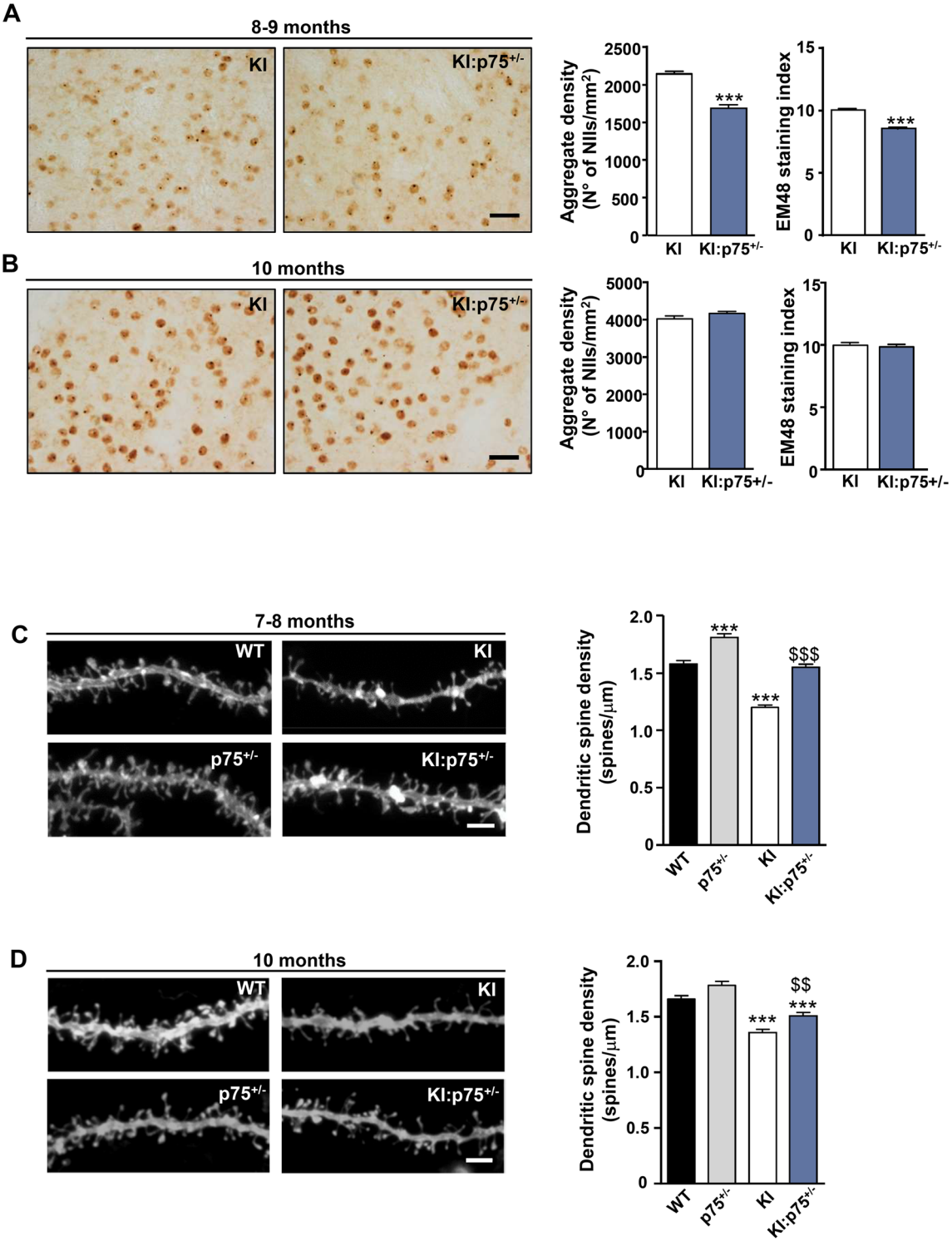

Fig. 3 Normalization of $p75^{NTR}$ expression in KI mice reduces mutant huntingtin aggregation and dendritic spine loss. Representative photomicrographs showing nuclear EM48 immunostaining in the dorsal striatum of 8–9-month-old (**a**) and 10-month-old (**b**) KI and KI:$p75^{+/-}$ mice. Scale bar 20 μm. Histograms represent density of $EM48^{+}$ neuronal intranuclear inclusions (NIIs) and "staining index," which captures both the nuclear staining intensity and the number of immunostained nuclei. Diffuse huntingtin immunostaining was lighter and surrounded the huntingtin aggregates. Data are shown as the mean ± SEM ($n = 600$–900 images from 3 to 4 mice). Data were analyzed by a two-tailed Student's t test. $^{***}P < 0.001$ compared with KI. Representative dendrites of medium spiny neurons from WT, $p75^{+/-}$, KI, and KI:$p75^{+/-}$ mice at 7–8 months (**c**) and 10 months of age (**d**). Scale bar 3 μm. Histograms show quantitative analysis of dendritic spine density per micrometer of dendritic length. Data are shown as the mean ± SEM (90–100 dendrites; $n = 4$–5 animals per genotype). Data were analyzed by one-way ANOVA followed by Tukey's test. $^{***}P < 0.001$ compared with WT; $^{\$\$}P < 0.01$ and $^{\$\$\$}P < 0.001$ compared with KI

(Supplemental Fig. 2). Altogether, these data suggest that normalization of $p75^{NTR}$ levels contributes to delay the onset of striatal neuropathology, in accordance with the delayed onset of motor deficits described above.

Normalization of $p75^{NTR}$ in the Striatum of KI Mice Delays the Reduction of BDNF/TrkB Expression

Survival and maintenance of MSNs are especially dependent on the BDNF-TrkB signaling pathway [5, 6]. Low striatal BDNF protein levels have been reported in postmortem HD brain samples and in several HD mouse models [7–10]. Moreover, we have demonstrated an imbalance of $p75^{NTR}$ and TrkB expression in mouse and human HD brain associated with increased striatal susceptibility [19]. Therefore, we have examined whether normalization of striatal $p75^{NTR}$ expression could affect BDNF and TrkB levels in the striatum. Total levels of BDNF (tBDNF) including both BDNF isoforms, the precursor proBDNF and the mature (m)BDNF, were assessed by ELISA (Fig. 4a), while only mBDNF was measured by Western Blot analysis (Fig. 4b). The specificity of the commercial anti-BDNF antibodies used in the study was validated by Western Blot using brain lysates from homozygous and heterozygous BDNF mice and recombinant BDNF as a positive control (Supplemental Fig. 3). In line with previous published data in other HD mouse models [7, 10], 8- and 10-month-old KI mice exhibited a robust reduction in striatal tBDNF levels analyzed by ELISA (Fig. 4a). Although this reduction in tBDNF could be attributed to a reduction in both BDNF isoforms, it has previously been shown that proBDNF is barely detectable in WT and HD striatum [10]. Importantly, decreased tBDNF levels could not be observed in KI:$p75^{+/-}$ mice until the age of 10 months with comparable tBDNF levels between KI:$p75^{+/-}$ and WT mice at 6 and 8 months of age. However, no statistical differences were detected between 8-month-old KI:$p75^{+/-}$ and KI (Fig. 4a). Interestingly, the observed decrease in tBDNF levels by ELISA correlates well with the significant reduction of mBDNF protein revealed by Western Blot in 8-month-old KI mice (Fig. 4b). Furthermore, a significant increase in mBDNF levels was observed in KI:$p75^{+/-}$ at 8 months but not at 10 months of age compared to KI mice (Fig. 4b), indicating that normalization of $p75^{NTR}$ levels delays mBDNF downregulation in KI:$p75^{+/-}$ mice. It is noteworthy that we observed a trend toward an age-dependent reduction of tBDNF levels in the four genotypes which is consistent with previous studies that have shown loss of BDNF gene transcription with aging [10, 38–41]. Since cortical afferents are the main source of striatal BDNF [42], we further evaluated mBDNF levels in cortical extracts from WT,

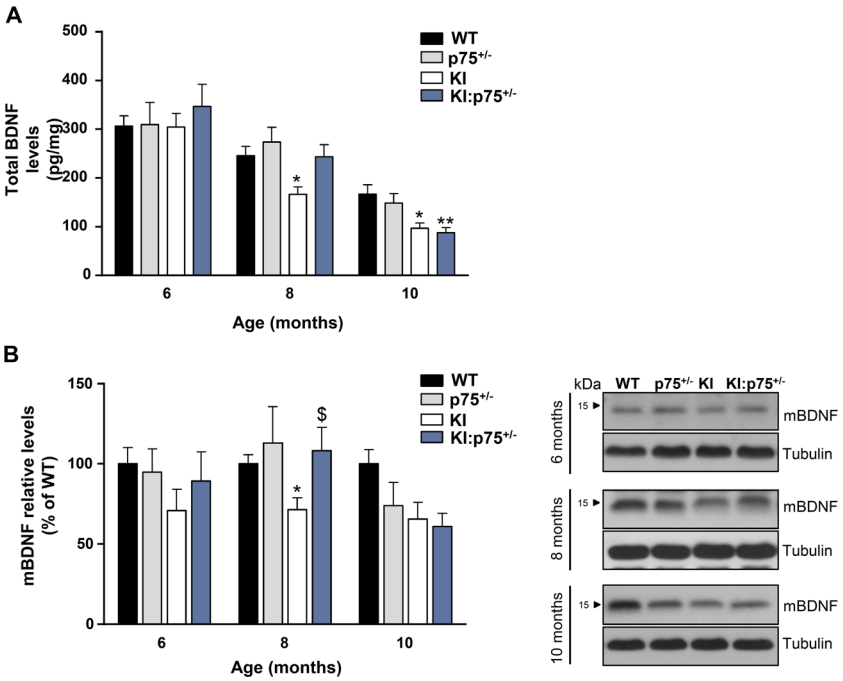

Fig. 4 Delayed reduction of striatal BDNF levels by normalization of $p75^{NTR}$ expression in KI mice. BDNF quantification was performed using striatal tissue obtained from WT, $p75^{+/}$, KI, and KI:$p75^{+/-}$ mice at 6, 8, and 10 months of age. **a** Histogram represents total BDNF levels expressed as picograms per milligram of protein obtained by ELISA. Data are expressed as the mean ± SEM ($n = 5$–7 mice/genotype/age). Data were analyzed at each age by one-way ANOVA followed by Tukey's test. $^{*}P < 0.05$ and $^{**}P < 0.01$ compared with WT. **b** Representative immunoblots showing the levels of mature BDNF (mBDNF) and tubulin as loading control in striatal extracts. Histograms represent the relative protein levels expressed as percentage of WT values. All data are shown as the mean ± SEM ($n = 5$–7 mice/genotype/age). Data were analyzed by one-way ANOVA followed by Tukey's test. $^{*}P < 0.05$ compared with WT; $^{\$}P < 0.05$ compared with KI

p75$^{+/-}$, KI, and KI:p75$^{+/-}$ at 6, 8, and 10 months of age (Supplemental Fig. 1B). Our results demonstrated unaltered mBDNF levels between genotypes at any of the evaluated ages suggesting that cortical mBDNF production is not affected neither by upregulation of p75^{NTR} in the striatum of KI mice nor by the genetic normalization of its levels in KI:p75$^{+/-}$. Similarly to striatal BDNF, a reduction in full-length TrkB levels was observed in KI mice from 8 months of age while such decrease could not be detected in KI:p75$^{+/-}$ mice until 10 months (Fig. 5a). No changes in the levels of the truncated TrkB isoform were observed (Fig. 5b). Next, activation of TrkB was analyzed by quantification of TrkB phosphorylation at tyrosine residues 816 (Y816), which lies within the C-terminus of TrkB-binding phospholipase C-gamma (PLCγ) and 515 (Y515), mediating SHC binding (Fig. 5c, d) [43]. A significant decrease in Y816 phosphorylation was found in KI mice at 8 months of age which could not be detected in KI:p75$^{+/-}$ mice until the age of 10 months (Fig. 5c). The levels of phosphorylated TrkB at the Y816 site in KI:p75$^{+/-}$ were significantly higher in comparison with KI mice at the age of 6 and 8 months. No significant differences on Y515 phosphorylation were found between genotypes (Fig. 5d). Taken together, these data indicate that BDNF-TrkB deficits along with altered TrkB phosphorylation status can be delayed in KI mice through normalization of p75^{NTR} levels.

Impaired TrkB-Induced Phosphorylation of PLCγ Can Be Delayed in KI Mice by Normalization of Striatal p75^{NTR} Levels

Since levels of TrkB and BDNF are decreased in the striatum of KI mice from 8 months of age, we evaluated the three major downstream signaling pathways associated with TrkB

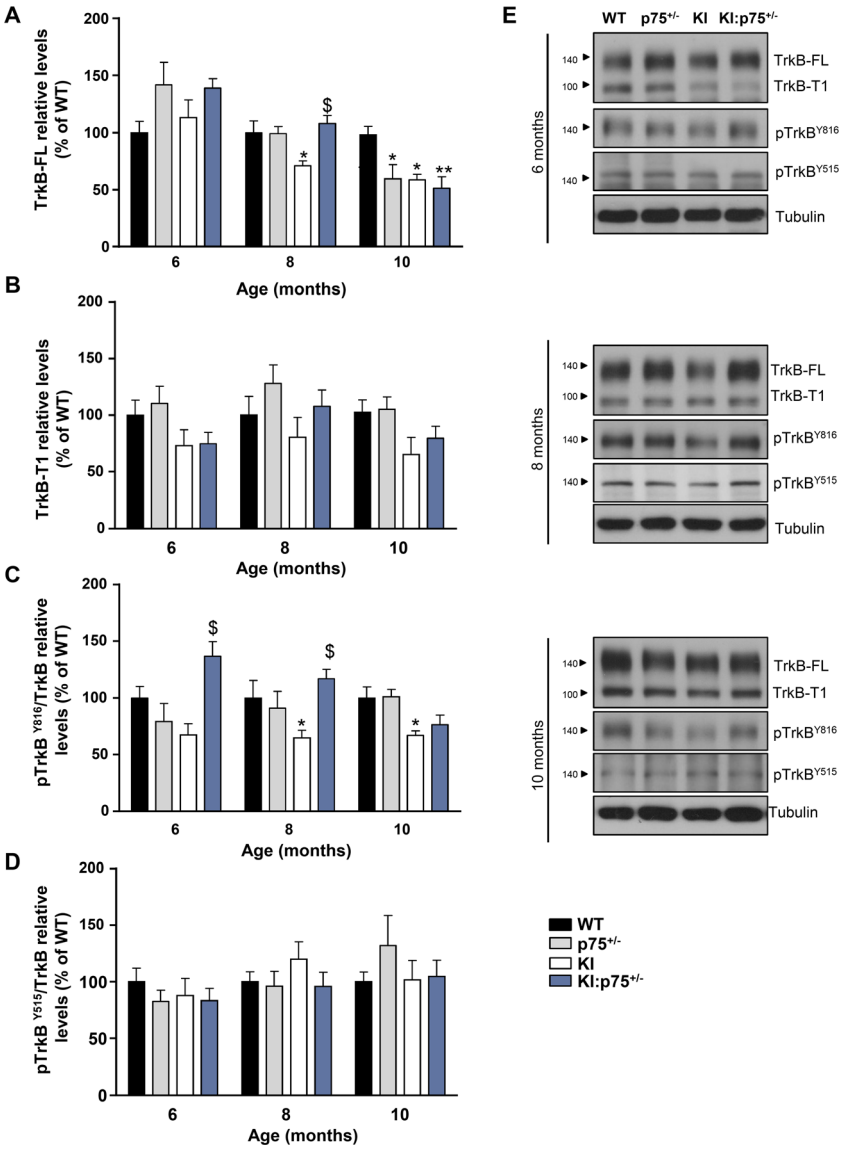

Fig. 5 Reduced expression and activation of TrkB can be delayed by normalization of p75^{NTR} expression in KI mice. Histograms represent the relative protein levels of TrkB full-length (TrkB-FL) (**a**) and TrkB truncated isoform (TrkB-T1) (**b**) with tubulin as loading control and the relatives ratios of phospho-TrkB (Y816)/TrkB (**c**) and phospho-TrkB (Y515)/TrkB (**d**) in striatal extracts obtained from WT, p75$^{+/-}$, KI, and KI:p75$^{+/-}$ mice at 6, 8, and 10 months of age. All data are shown as percentage of WT values and represented as the mean ± SEM ($n = 5$–7 mice/genotype/age). Data were analyzed by one-way ANOVA followed by Tukey's test. *$P < 0.05$ and **$P < 0.01$ compared with WT; $^{\$}P < 0.05$ compared with KI. **e** Representative immunoblots from **a** to **d**

activation: PI3K/Akt, MAP/ERK1/2, and PLC/PKC [44]. Western Blot analysis of striatal tissue at different ages revealed an increased activation of Akt at 8 and 10 months of age in KI mice (Fig. 6a). This sustained Akt activation is consistent with previous results shown in knock-in and transgenic HD mouse models [45] and has been considered a pro-survival mechanism associated to reduced levels of PHLPP1 phosphatase [46] and to an abnormal NMDA receptor activation [47]. No changes in ERK activation were observed in the striatum of KI mice until the age of 10 months, when a slight but not significant decrease was observed (Fig. 6b). Importantly, a significant reduction on PLCγ activation was present from 6 months of age (Fig. 6c). Because aberrant levels or activation of $p75^{NTR}$ can alter TrkB signaling [24], we also investigated these pathways in KI:$p75^{+/-}$ mice. pAkt and pERK levels where comparable between KI and KI:$p75^{+/-}$ mice, indicating that these pathways are not affected by normalization of $p75^{NTR}$ levels (Fig. 6a, b). In contrast, reduced pPLCγ levels were restored in KI:$p75^{+/-}$ mice at 6 and 8 months but not at 10 months of age, when phosphorylation of PLCγ was reduced to similar levels of KI mice (Fig. 6c). Since Akt, ERK, and PLCγ pathways via TrkB signaling have been shown to phosphorylate CREB, promoting transcription of its target genes, such as BDNF, we also evaluated phosphorylation levels of CREB. However, no differences were observed between genotypes at any age evaluated (Supplemental Fig. 4). Altogether, these data demonstrate that normalization of $p75^{NTR}$ levels in the striatum of KI mice delays the deficient activation of PLCγ induced by TrkB.

Normalization of $p75^{NTR}$ in the Striatum of KI Mice Delays the Upregulation of JNK Activation

Activation of cell death signaling pathways, including JNK upregulation, has previously been reported in different HD models by our group and others [48–50]. Given that $p75^{NTR}$-mediated neurodegeneration has been associated with JNK activation [24], we next examined whether normalization of $p75^{NTR}$ levels in KI mice was accompanied by a reduction in JNK phosphorylation. Western Blot analysis of striatal extracts from WT, $p75^{+/-}$, KI, and KI:$p75^{+/-}$ mice revealed a significant increase in pJNK levels at 8 and 10 months of age in KI mice but not in KI:$p75^{+/-}$ animals, although no significant differences were observed between KI and

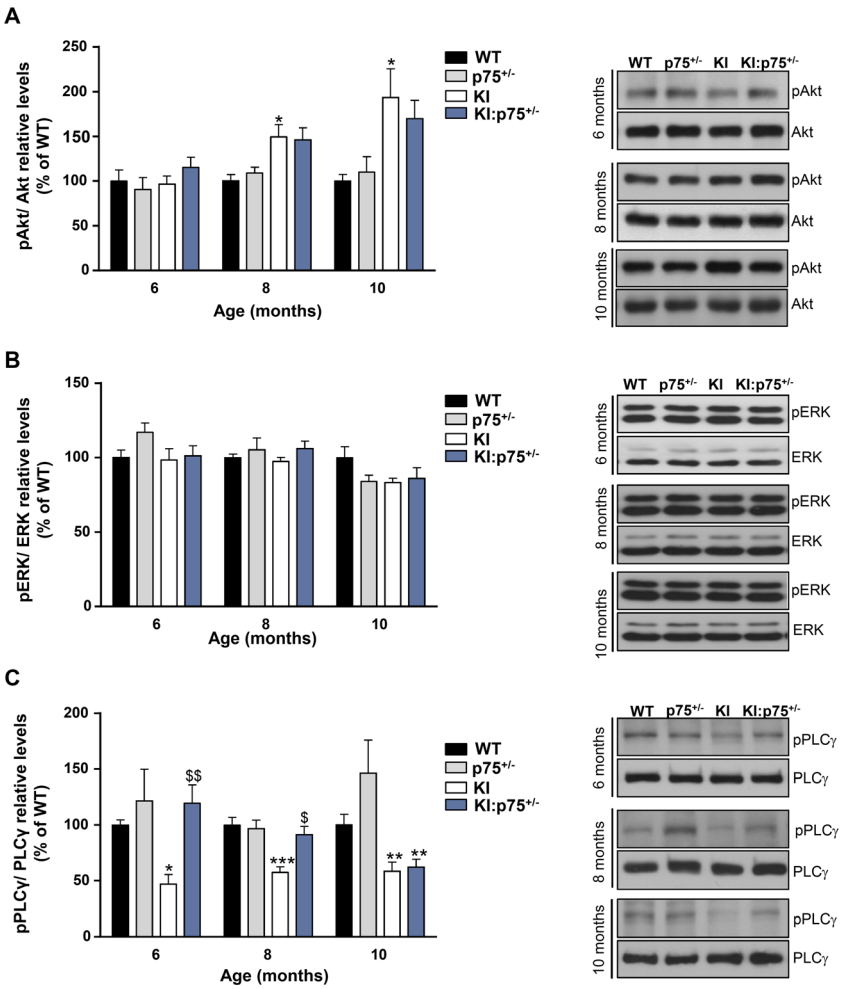

Fig. 6 Impaired PLCγ activation can be delayed by normalization of $p75^{NTR}$ expression in KI mice. Representative immunoblots showing the levels of pAkt and Akt (**a**), pERK and ERK (**b**), and pPLCγ and PLC γ (**c**) in striatal extracts obtained from WT, $p75^{+/-}$, KI, and KI:$p75^{+/-}$ mice at 6, 8, and 10 months of age. The histograms represent the relative pAkt/Akt, pERK/ERK and pPLCγ/PLCγ ratios expressed as percentage of WT values. All data are shown as the mean ± SEM ($n = 5$–7 mice/genotype/age). Data were analyzed by one-way ANOVA followed by Tukey's test. *$P < 0.05$, **$P < 0.01$, and ***$P < 0.001$ compared with WT; $^{\$}P < 0.05$ and $^{\$\$}P < 0.01$ compared with KI

KI:p75$^{+/-}$ (Fig. 7a). Since JNK activation mediates direct phosphorylation of its substrate c-Jun, we assessed levels of phospho-c-Jun (Ser63) (pc-Jun) by Western Blot analysis. A significant increase in this pro-apoptotic transcription factor was detected at 10 months of age in KI mice while only a trend was observed at 6 and 8 months (Fig. 7b). Interestingly, pc-Jun was significantly reduced at 6 and 8 months in KI:p75$^{+/-}$ mice in comparison with KI mice. To determine whether reduced JNK activation was also associated with inhibition of caspase-3 activity, the caspase-3 cleaved spectrin fragment SBDP120 was analyzed by Western Blot. No significant changes in SBDP120 levels were found between genotypes (Fig. 7c). These findings indicate that activation of JNK apoptotic pathway can be partially prevented by normalization of p75^{NTR} expression in KI mice. Despite the activation of these death signaling pathways, it is widely accepted that the Hdh$^{Q7/Q111}$ mouse model is spared of evident neuronal loss. Indeed, we found no cleaved caspase-3 positive-stained cells in corticostriatal slices from WT and KI mice (Supplemental Fig. 5), which confirms previous studies showing unaltered NeuN+ neuronal density in the striatum of Hdh$^{Q7/Q111}$ mice for up to 12 months [51]. Supporting the lack of neurodegeneration in this HD mouse model, no changes in cortical thickness were neither observed between genotypes (Supplemental Fig. 6). Overall, these results showing no neuronal death in our Hdh$^{Q7/Q111}$ HD model indicate that the early increase in p75^{NTR} levels could lead to neuronal dysfunction without affecting cell viability.

Chronic Administration of Fingolimod Prevents TrkB/p75^{NTR} Imbalance and Ameliorates Neuropathology in the Striatum of R6/1 Mice

We have previously demonstrated that chronic treatment with fingolimod (FTY720), a sphingosine-1 phosphate receptor modulator, prevented the reduction of TrkB and BDNF levels

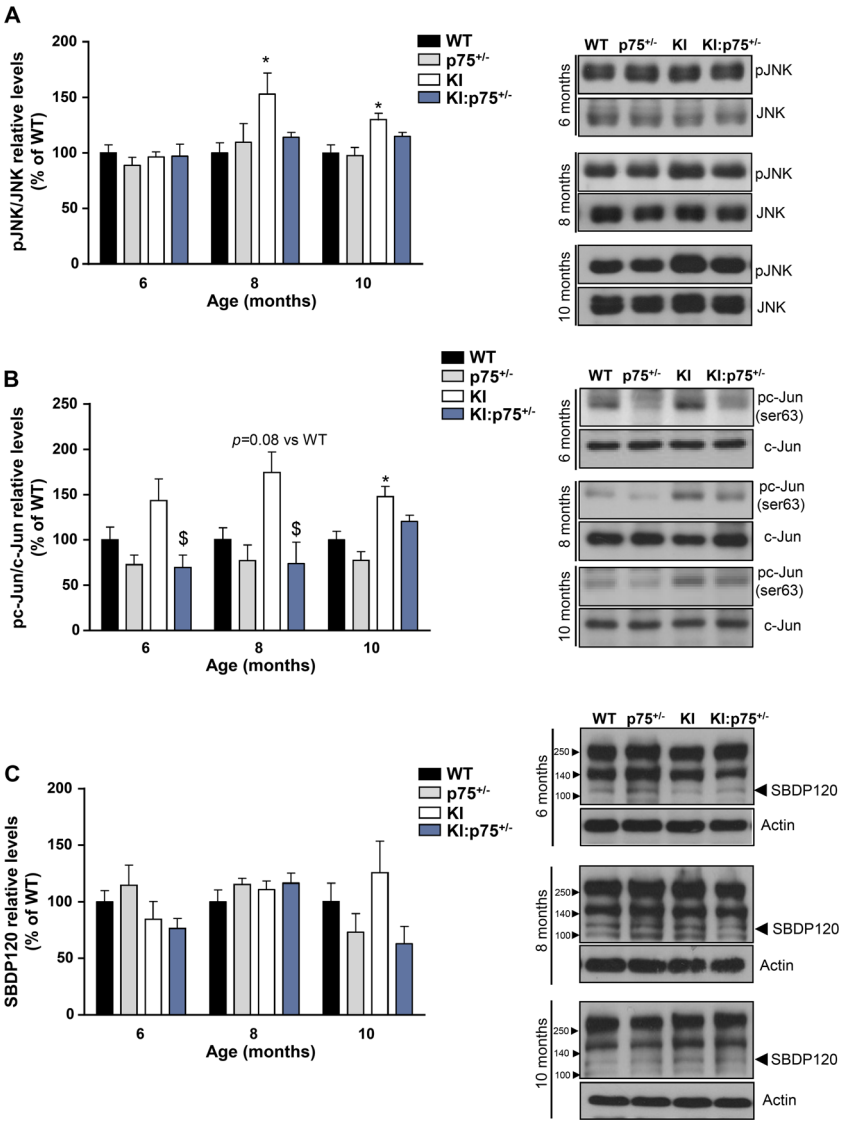

Fig. 7 Normalization of p75^{NTR} in KI mice attenuates activation of JNK. Representative immunoblots showing the levels of pJNK and JNK (**a**), pc-Jun and c-Jun (**b**), and αII-spectrin breakdown product 120 (SBDP120) (**c**) with tubulin as loading control in striatal extracts obtained from WT, p75$^{+/-}$, KI, and KI:p75$^{+/-}$ mice at 6, 8, and 10 months of age. Histograms represent the relative ratios of pJNK/JNK and pc-Jun/c-Jun and the relative levels of SBDP120 expressed as percentage of WT values. All data are shown as the mean ± SEM ($n = 5$–7 mice/genotype/age). Data were analyzed by one-way ANOVA followed by Tukey's test. *$P < 0.05$ compared with WT; $^{\$}P < 0.05$ compared with KI

and normalized the expression of $p75^{NTR}$ in the hippocampus of R6/1 transgenic mice [29]. Given that genetic normalization of striatal $p75^{NTR}$ expression delays BDNF/TrkB/$p75^{NTR}$ signaling alterations and improve neuropathology, we wondered whether FTY720 administration was also able to prevent striatal pathology in HD mice. To this aim, we used the R6/1 mouse model that displays earlier onset and faster disease progression than KI mice and presents a good correlation between the onset of motor impairments [52] and the upregulation of $p75^{NTR}$ in the striatum at 12 weeks of age [19]. Mice were treated with FTY720 from presymptomatic (8 weeks) to symptomatic (20 weeks) stages, when R6/1 mice manifest overt motor and cognitive behavioral deficits. In agreement with previous findings [11, 19, 53, 54], R6/1 mice at the age of 20 weeks did not show reduced levels of mature BDNF and full-length TrkB but a trend toward an increase in $p75^{NTR}$ protein levels ($P = 0.052$; Fig. 8a). Notably, treatment with FTY720 completely prevented $p75^{NTR}$ upregulation, showing R6/1-treated mice similar levels of $p75^{NTR}$ compared with WT mice. These results demonstrate that chronic administration of FTY720 prevents the TrkB/$p75^{NTR}$ imbalance in the striatum of HD mice. Next, we analyzed whether normalization of this imbalance could ameliorate striatal neuropathology. The presence of mHtt aggregates was evaluated by immunohistochemical analysis. Treatment with FTY720 significantly decreased the number of EM48 positive nuclear inclusions (Fig. 8b). Moreover, in accordance with the partial recovery of DARPP32 expression observed in the striatum of KI:$p75^{+/-}$ mice (Fig. 2a), FTY720 treatment also prevented DARPP32 reduction, as shown by the increase in protein levels exhibited by FTY720-treated R6/1 mice compared with vehicle-treated animals (Fig. 8c). Altogether, these data demonstrate that regulation of $p75^{NTR}$ levels by therapeutic strategies like FTY720 can maintain BDNF/TrkB/$p75^{NTR}$ balance preventing striatal neuropathology.

Chronic Administration of Fingolimod Ameliorates Motor Coordination Deficits in R6/1 Mice

We have previously demonstrated that genetic normalization of $p75^{NTR}$ expression delays the onset of motor coordination deficits in KI mutant mice. Given that FTY720 treatment restores the balance between TrkB and $p75^{NTR}$ expression in R6/1 mice, we next assessed the potential of FTY720 to prevent or ameliorate motor abnormalities. Behavioral analysis using the rotarod at 24 rpm revealed that R6/1 mice start showing significant differences from WT mice at 14 weeks of age (Fig. 8d). Remarkably, the beneficial effects of the compound on motor function and coordination were first observed at this age, after 6 weeks of treatment (Fig. 8d). Chronic infusion of FTY720 significantly improved the rotarod performance of R6/1 manifested as a decrease in the number of falls compared with vehicle-treated R6/1 mice. No significant differences were observed between vehicle- and FTY720-treated WT mice. Overall, these results indicate that HD striatal neuropathology and motor coordination disturbances are dependent on the balance between TrkB and $p75^{NTR}$ expression.

Discussion

The present study demonstrates the critical contribution of the BDNF/TrkB/$p75^{NTR}$ pathway to the onset of motor deficits and striatal neuropathology in HD mice. Longitudinal motor behavioral evaluation of full-length HD mice reveals a correlation between the onset of motor coordination abnormalities, the reduction in BDNF and TrkB levels, and the increase in $p75^{NTR}$ protein levels. Accordingly, genetic normalization of $p75^{NTR}$ expression in KI mutant mice delayed the onset of motor deficits and striatal dysfunction likely by restoring the balance between BDNF/TrkB/$p75^{NTR}$ expression and signaling. It is important to keep in mind that KI and R6/1 mice show increased levels of $p75^{NTR}$ in the striatum and hippocampus but not in the cortex [28]. This finding supports our hypothesis that the normalization of $p75^{NTR}$ in the striatum of KI mice is the responsible of the delay in motor deficits. Similarly, as previously reported by our group, hippocampal memory and synaptic plasticity deficits in KI mice can be prevented by the genetic downregulation of $p75^{NTR}$ in the hippocampus [28]. Furthermore, we also found that chronic pharmacological treatment with fingolimod improved motor behavior and striatal neuropathology in HD transgenic mice by normalizing $p75^{NTR}$ protein levels and therefore correcting the BDNF/TrkB/$p75^{NTR}$ imbalance.

Deficits of neurotrophic support to striatal neurons in HD have recently been associated not only to reduced levels of BDNF but also to impaired BDNF signaling and altered expression of BDNF receptors [17, 19–21, 30]. Besides these new pieces of evidence, no studies so far have explored the contribution of deficient BDNF signaling or impaired balance of BDNF receptors (TrkB and $p75^{NTR}$) to the onset of motor coordination deficits. To address this question, we have used double-mutant mice in which $p75^{NTR}$ expression has been normalized and we have evaluated many outcome measures such as motor coordination, striatal pathology and biochemical analysis along disease progression. Although in some measures 8-month-old KI:$p75^{+/-}$ mice did not perform significantly better than the KI, they did not show significant differences compared with WT neither. Then, our results show that normalization of $p75^{NTR}$ expression in KI mice delays from 6 to 10 months of age the onset of motor coordination deficits and striatal pathology, as well as the reduction in TrkB and BDNF protein levels. Interestingly, downregulation of $p75^{NTR}$ levels at 10 months of age fails to prevent striatal neuronal dysfunction and loss of motor coordination in KI mice most likely

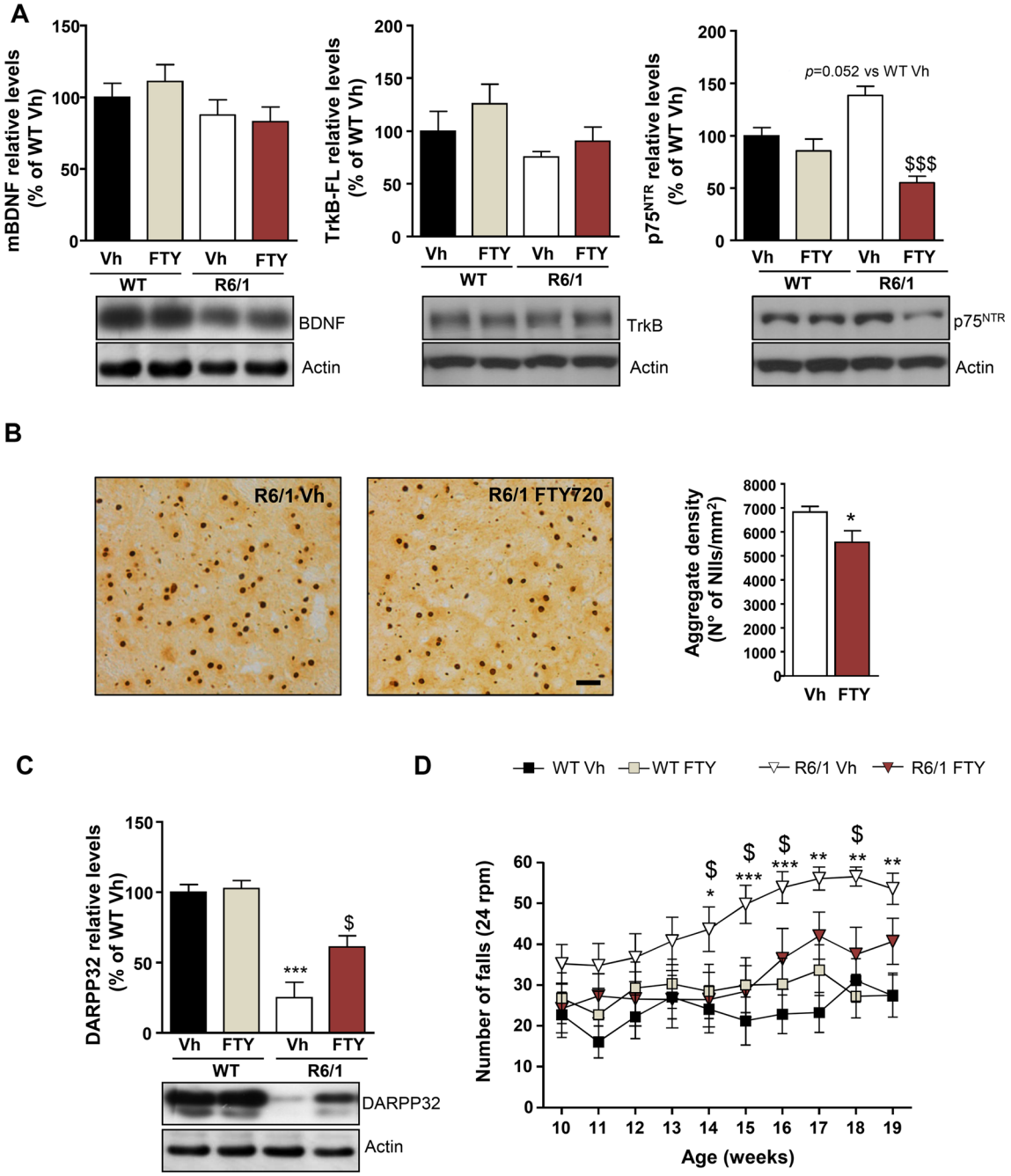

Fig. 8 Fingolimod (FTY720) chronic treatment reduces $p75^{NTR}$ expression levels and prevents motor deficits and striatal pathology in R6/1 mice by **a** representative immunoblots showing the levels of mature BDNF (mBDNF), full-length TrkB (TrkB-FL), $p75^{NTR}$, and β-actin as loading control in striatal extracts of WT and R6/1 mice, after either vehicle or FTY720 chronic administration. Histograms represent protein levels expressed as percentage of WT vehicle. All data are shown as the mean ± SEM ($n = 5$–6 mice/genotype/treatment). Data were analyzed by one-way ANOVA followed by Tukey's test. $^{\$\$\$}P < 0.001$ compared with vehicle-treated R6/1 mice. **b** Representative photomicrographs showing nuclear EM48 immunostaining in the striatum of 20-week-old R6/1 mice treated with vehicle or FTY720. Scale bar 50 μm. Histograms represent the density of $EM48^+$ of neuronal intranuclear inclusions (NIIs) per square millimeter. Data are expressed as the mean ± SEM ($n = 6$ mice/treatment). Data were analyzed by a two-tailed Student's *t* test. $^{*}P < 0.05$ compared with vehicle-treated R6/1mice. **c** Western Blot analysis of DARPP32 and β-actin as loading control in striatal extracts from WT and R6/1 mice, after vehicle or FTY720 chronic administration. Histogram represents relative protein levels expressed as the percentage of WT vehicle. All data are shown as the mean ± SEM ($n = 5$–6 mice/genotype/treatment). Data were analyzed by one-way ANOVA followed by Tukey's test. $^{***}P < 0.001$ compared with vehicle-treated WT mice; $^{\$}P < 0.05$ compared with vehicle-treated R6/1 mice. **d** The number of falls from a fixed speed rotarod were recorded during 60 s at 24 rpm every week from 10 to 19 weeks of age. Data are expressed as the mean ± SEM ($n = 10$–12 animals/genotype/treatment). Data were analyzed by two-way ANOVA with repeated measures followed by Tukey's test. $^{*}P < 0.05$, $^{**}P < 0.01$, $^{***}P < 0.001$: vehicle-treated R6/1 mice compared with vehicle-treated WT mice; $^{\$}P < 0.05$: FTY-treated R6/1 mice compared with vehicle-treated R6/1 mice

because the reduction in TrkB and BDNF levels can no longer be blocked. These results suggest that a correct balance in BDNF/TrkB/p75^{NTR} levels is critical to support the neurotrophic signaling in medium spiny neurons (MSNs) needed to control motor function. Certainly, it is well known that the survival, maintenance, and function of MSNs are particularly dependent on the BDNF-TrkB signaling pathway [5, 6]. Consistently, key striatal-enriched proteins such as DARPP32, A2AR, and PDE10A whose expression is reduced in HD [32–34] were preserved as long as the BDNF/TrkB/p75^{NTR} imbalance was prevented. Importantly, the function of these proteins is critical to regulate striatonigral and striatopallidal downstream signaling cascades that work for the fine-tuning of movement [55–57]. Thus, A2AR is required for most of the synaptic functions of BDNF/TrkB [58–60] while DARPP32, a key integrator of dopamine and glutamate neurotransmission in MSNs [61–63], participates through interaction with adducin to modulate dendritic spine stability [64]. Indeed, in our double-mutant KI:p75$^{+/-}$ mice, normalization of p75^{NTR} levels prevented the loss of striatal dendritic spines. Altogether, these findings support the idea that abnormalities in the BDNF/TrkB/p75^{NTR} signaling may contribute to reduce the expression of key striatal proteins leading to neuronal dysfunction and subsequent motor deficits in HD. As previously discussed, BDNF/TrkB pathway and striatal integrity cannot be restored by normalization of p75^{NTR} at late disease stages in KI:p75$^{+/-}$, probably due to other pathological mechanisms triggered by mutant huntingtin, such as progressive transcriptional alterations, which have been already described in our Hdh$^{Q7/Q111}$ mouse model [51].

It remains unclear how the increment in p75^{NTR} found in the striatum and the consequent restoration in the double-mutant mice can affect striatal mBDNF. In agreement with our results, several studies have described decreased striatal mBDNF levels without cortical BDNF alterations [11, 65, 66]. These results suggested that anterograde transport of mBDNF and/or proBDNF from cortex to striatum could be impaired [8, 67]. Since it is well known that p75^{NTR} is involved in axonal degeneration [68], it is possible to hypothesize that normalization of p75^{NTR} in HD mice could contribute to reduce the axonal pathology in corticostriatal connections present in HD mice [69, 70] and restore BDNF transport. Further studies would be necessary to elucidate this potential mechanism.

Beyond the observed alterations of BDNF and TrkB protein levels, we found that the onset of motor deficits and the reduction of striatal-enriched proteins in KI mice were also associated with a specific decrease in TrkB-PLCγ signaling. Thus, in line with previous studies in other HD mouse models [10, 53], reduced phosphorylation of PLCγ and TrkB at Y816, the tyrosine residue associated with PLCγ activation, was observed in KI mice along the disease progression. In contrast, TrkB phosphorylation at Y515 remained unchanged between genotypes. This differential phosphorylation of TrkB tyrosine residues could be the result of BDNF-independent molecular mechanisms already described in several studies [71–74]. Interestingly and consistent with a delay in motor dysfunction, impaired TrkB-PLCγ signaling was also delayed by normalization of p75^{NTR} levels. This data might be explained by the restored BDNF levels observed in double-mutant KI:p75$^{+/-}$ mice and/or by a direct effect of p75^{NTR} on TrkB phosphorylation sites. Indeed, previous studies have already reported attenuation of BDNF-mediated autophosphorylation of TrkB by p75^{NTR} [75] and increased TrkB phosphorylation has been observed under p75^{NTR} masking conditions in hippocampal neurons [76]. Evidence showing that p75^{NTR} directly interacts with Trk receptors [77] leads to speculate that binding of BDNF to p75^{NTR} directly affects conformation and, therefore, the affinity of TrkB for BDNF. However, this crosstalk between p75^{NTR} and TrkB receptor affecting BDNF signaling in HD needs to be further explored.

Altered neuronal function in different brain disorders has been associated with abnormal activation of PLCγ resulting in impaired neuronal activity and ultimately cell death [78]. In our HD model, reduced PLCγ activity might contribute to striatal pathology by decreasing striatal protein markers such as DARPP32 [5, 79] and A2AR [80]. On the other hand, due to the role of PLCγ signaling in the functional changes of spine actin cytoskeleton [81–83], the decreased striatal spine density detected in mutant KI mice could be a consequence of PLCγ activity downregulation.

Besides the recovery of the pro-survival signaling pathway PLCγ following normalization of p75^{NTR} expression, we also demonstrated reduced activation of the pro-apoptotic JNK pathway. Based in our previous published data showing that the increase in p75^{NTR} levels is associated with DARPP32+ striatal neurons [19], we can hypothesize that the observed increase in JNK activation could also occur in these neurons. It is noteworthy that even though in the p75$^{+/-}$ heterozygous mice a dose-dependent effect of p75^{NTR} gene copy number on pJNK levels would be expected, we observed that p75$^{+/-}$ mice mostly display phenotypes similar to WT. We hypothesize that the activation or inhibition of specific pathways are dependent on an "optimal range" of p75^{NTR} expression levels. Moreover, we cannot exclude that additional pathways could regulate JNK activation since p75^{NTR} levels are increased at 6 months of age in KI mice striatum but JNK activity is unaltered at this age. The involvement of JNK in mHtt-mediated striatal neurotoxicity is supported by a number of different in vitro and in vivo studies [48–50]. Activation of cellular stress response manifested as JNK phosphorylation has been reported in cells expressing polyglutamine aggregates while inhibition of JNK activation slowed and reduced the formation of such polyQ-protein aggregates [84–86]. In this view, we propose that attenuation of JNK signaling activation by normalization of p75^{NTR} expression might also contribute to reduce the number of intranuclear mHtt aggregates observed in the striatum of

double-mutant KI:p75$^{+/-}$ mice. Indeed, it has been recently shown that modulation of p75^{NTR} by small molecules that specifically enhances pro-survival downstream signals and inhibits pro-apoptotic JNK activation ameliorates HD striatal pathology [30]. Moreover, JNK activation has also been shown to mediate the inhibitory effect of mutant huntingtin on axonal transport [87]. Therefore, the present data showing JNK activity downregulation underlying the beneficial effect of p75^{NTR} normalization on KI mice pathology might explain why a variety of therapies based on neurotrophic factors partially improve mutant huntingtin-induced pathology in other mouse HD models. Nevertheless, we cannot exclude that other pathways associated with p75^{NTR} signaling, like RhoA/ROCK cascade [23, 25], could also be involved. Aberrant activity of p75^{NTR} in HD mice increases RhoA activation leading to impaired synaptic plasticity [20, 28, 29], and importantly, inhibition of the ROCK pathway enhances mHtt degradation and reduces aggregation while improving motor function in R6/2 mice [88–91]. These findings suggest that the reduction of mHtt aggregates could be due to the inhibition of JNK, as well as RhoA/ROCK signaling, once levels of p75^{NTR} are normalized.

We further confirmed the critical contribution of the proper balance of BDNF/TrkB/p75^{NTR} to motor deficits in HD mice by using a pharmacological approach. Fingolimod (FTY720) is an immunomodulator known to improve BDNF release in the striatum, to rescue motor deficits in mouse models of Rett's syndrome and HD [93, 92], and to prevent cognitive deficits and imbalance of BDNF receptors in the hippocampus of R6/1 mice [29]. Chronic administration of fingolimod improved motor function in 20-week-old R6/1 mice, reduced mHtt aggregates and increased DARPP32 expression, in agreement with previous data in R6/2 mice [93]. Notably, FTY720 treatment also normalized p75^{NTR} levels, aberrantly expressed in R6/1 mice between 12 and 30 weeks of age [19]. BDNF levels were not found significantly decreased in the striatum of R6/1 mice at 20 weeks of age. While this finding is consistent with previous reports [54], other studies have found decreased BDNF mRNA or protein levels at the same age analyzed [66, 94]. The addition of behavioral tasks prior to obtaining samples, the use of different genetic backgrounds, or the diversity in commercial antibodies against BDNF could account for the observed different results. No changes in TrkB levels at 20 weeks of age between WT and R6/1 mice were observed neither, consistent with previous studies reporting downregulation at 30 weeks of age [19]. We cannot rule out that other mechanisms modulated by FTY720 might contribute to the therapeutic benefits observed in R6/1 mice. Indeed, it has been demonstrated that FTY720 can increase phosphorylation of mutant huntingtin at serine 13/16 residues to attenuate protein toxicity [93], as well as modulate CREB expression [92] or inhibit class I histone deacetylases (HDACs) in neurons [95]. Nevertheless, based on our findings, we hypothesize that the improvement in motor coordination observed in FTY720-treated R6/1 mice can be mainly attributed to prevention of BDNF/TrkB/p75^{NTR} imbalance.

It can be argued that the genetic or pharmacological normalization of p75^{NTR} is not exclusively neuronal since expression of p75^{NTR} in astrocytes has been reported following different brain injuries [96, 97]. However, we have previously demonstrated that the aberrant p75^{NTR} increase in the striatum and the hippocampus of the Hdh^{Q111} mice is neuron-specific [19, 28], supporting the idea that normalization of p75^{NTR} contributes to restore BDNF/TrkB signaling in neurons.

In conclusion, this work shed new light on how the imbalance of the BDNF/TrkB/p75^{NTR} system can affect striatal neuropathology and motor behavior in HD. It demonstrates that this imbalance leads to impaired BDNF signaling trough reduced TrkB-PLCγ pathway and increased JNK activation. More importantly, we show that normalization of p75^{NTR} expression delays such impairments that follow the well-described "dying back" pattern of neuronal degeneration in HD [98]. Our study further supports the role of p75^{NTR} signaling in striatal pathophysiology highlighting the potential benefits of restoring BDNF/TrkB/p75^{NTR} balance for preventing, delaying, or reversing the progression of HD pathology.

Methods

Animals Heterozygous HdhQ111 knock-in mice (KI) [99] and p75$^{+/-}$ heterozygous mice (p75^{NTR}/ExonIII) from the Jackson Laboratory were bred. KI and p75$^{+/-}$ were C57BL/6 genetic background. Only males from each genotype, Hdh$^{Q7/Q7}$ (WT), Hdh$^{Q7/Q111}$ (KI), p75$^{+/-}$, and KI:p75$^{+/-}$, were used for all experiments. Male R6/1 transgenic mice (B6CBA background) expressing the exon-1 of mutant huntingtin with 145 repeats were used for pharmacological experiments [100]. Male C57BL/6J (WT) mice, BDNF$^{+/-}$ mice, and BDNF$^{-/-}$ from the Jackson Laboratory were bred and used to test specificity of BDNF antibodies. Experimental procedures were approved by the Local Ethical Committee of the University of Barcelona (99/01) and the Generalitat de Catalunya (00/1094), following European (2010/63/UE) and Spanish (RD 1201/2005) regulations for the care and use of laboratory animals.

Drug Administration FTY720 was obtained as a powder from Cayman Chemicals and dissolved in EtOH 10% in distilled water (vehicle). For chronic pharmacological treatment, intraperitoneal injections of FTY720 were given every 4 days at a dose of 0.3 mg/kg for 12 weeks, starting at 8 weeks of age. Animals were weighted weekly in order to determine the appropriate dose. Mice were distributed into four experimental groups (n = 10–12 each): WT + FTY720, WT + vehicle, R6/1

+ FTY720, and R6/1 + vehicle. Last dose of FTY720 was administered 24 h before sacrificing the animals for histological and biochemical analysis.

Behavioral Assessment

Fixed Rotarod Motor coordination and balance were evaluated on the rotarod apparatus at distinct rotations per minute (rpm), as described elsewhere [54]. In brief, KI mice (5–6 months old) and R6/1 mice (7 weeks old) were trained at constant speed (10 rpm) for 60 s. We performed two trials per day for three consecutive days, and the latency to fall and the number of falls during 60 s was recorded. No differences between groups were detected at this period. After training and starting at 7 months of age, KI mice were evaluated once a month at 10 and 24 rpm until 12 months of age, and the number of falls in a total of 60 s was recorded. R6/1 mice were evaluated at 24 rpm, once a week, from 10 to 19 weeks of age. The animals were put on the rotarod several times until the addition of the latency to fall off reached a total of 60 s.

Open Field Independent cohorts of 8- and 10-month-old WT, KI, $p75^{+/-}$, and KI:$p75^{+/-}$ animals (only males) were used. The device consisted of a white circular arena with 40 cm diameter and 40 cm high. The light intensity was 40 lx throughout the arena, and the room temperature was kept at 19–22 °C and 40–60% humidity. Mice were placed into the arena during two consecutive days (15 min/day), and spontaneous locomotor activity was measured as total distance traveled. The arena was rigorously cleaned between animals in order to avoid odors. Animals were tracked and recorded with SMART Junior Software.

Western Blotting WT and HD mice were killed by cervical dislocation, and the brains were quickly removed, dissected, frozen in dry ice, and stored at − 80 °C until use. Protein extracts were prepared from striatal brain samples by sonication on ice for 10 s in lysis buffer containing 50 mM Tris base (pH 7.4), 150 mM NaCl, 0.1 mM phenylmethylsulfonyl fluoride, and 1% NP-40 supplemented with 1 mM sodium orthovanadate and protease inhibitor mixture (Sigma-Aldrich). Samples were centrifuged at 10,000×*g* for 10 min, and the protein contents determined by Detergent-Compatible Protein Assay (bicinchoninic acid, BCA; Bio-Rad). Protein extracts (30 μg) were mixed with 4× SDS sample buffer, boiled for 5 min, resolved by 8–12% SDS-polyacrylamide gel electrophoresis, and transferred to nitrocellulose membranes (Schleicher & Schuell). Blots were blocked in 10% non-fat powdered milk in Tris-buffered saline Tween-20 (50 mM Tris-HCl, 150 mM NaCl, pH 7.4, 0.05% Tween-20) for 1 h at room temperature. The membranes were then incubated overnight at 4 °C with primary antibodies: anti-DARPP32 (1:1000, BD Biosciences, cat. no. 611520), anti-PDE10A (1:1000, Abcam, cat. no. ab14622), anti-A2AR (1:1000, Santa Cruz, cat. no. sc-32261), anti-BDNF (1:1000, Santa Cruz, cat. no. sc-546), anti-BDNF (1:1000, Icosagen, cat. no. 327-100, Clone 3C11), anti-$p75^{NTR}$ (1:1000, Promega, cat. no. G3231), anti-phospho-TrkB (Tyr816) (1:1000, Abcam, cat. no. ab75173), anti-phospho-TrkB (Tyr515) (1:1000, Abcam, cat. no. ab131483), anti-TrkB (1:1000, BD Biosciences, cat. no. 610101), anti-phospho-Akt (Ser473) (1:1000, Cell Signaling, cat. no. 3787), anti-Akt (1:1000, Cell Signaling, cat. no. 2920), anti-phospho p44/42 ERK1/2 (Thr202/Tyr204) (1:1000, Cell Signaling, cat. no. 9101), anti-ERK1/2 (1:2500, BD Biosciences, cat. no. 610123), anti-phospho-PLCγ1 (Tyr783) (1:1000, Cell Signaling, cat. no. 2821), anti-PLCγ1 (1:1000, Cell Signaling. cat. no. 2822), anti-phospho-CREB (Ser133) (1:1000, Millipore, cat. no. 06-519), anti-CREB (1:1000, Cell Signaling, cat. no. 9197), anti-phospho-SAPK/JNK (Thr183/Tyr185) (1:1000, Cell Signaling, cat. no. 9251), anti-SAPK/JNK (1:1000, Cell Signaling, cat. no. 9252), anti-phospho-c-Jun (Ser63) (Santa Cruz, 1:1000, cat. no. sc-822), anti c-Jun (Santa Cruz, 1:1000, cat. no. sc-74,543), anti-spectrin (1:1000, Chemicon, cat. no. MAB1622), anti-α-tubulin (1:50,000, Sigma-Aldrich, cat. no. T9026), and anti-actin (1:20,000, MP Biomedicals, cat. no. 69100). Membranes were then rinsed three times with Tris-buffered saline Tween-20 (TBS-T) and incubated with horseradish peroxidase-conjugated secondary antibody for 1 h at room temperature. After washing for 30 min with TBS-T, membranes were developed using the enhanced chemiluminescence substrate kit (Santa Cruz Biotechnology). Gel-Pro densitometry program (Gel-Pro Analyzer for Windows version 4.0.00.001) was used to quantify the different immunoreactive bands relative to the intensity of the α-tubulin or actin band in the same membranes. Data are expressed as the mean ± SEM of band density obtained in independent experiments or sample.

BDNF Immunoassay BDNF quantification was performed using an ELISA as previously described [101], with minor modifications. In brief, 96-well white polystyrene plates (Nunc) were coated with 1 μg of anti-BDNF #1 antibody in 100 μl carbonate buffer (pH 9.7) per well overnight at 25 °C. Plates were blocked with 4% BSA in PBS and washed three times with TBST. Samples and standards (1–1024 pg of recombinant purified BDNF per well) supplemented with 1% BSA and 1% NP-40 were incubated for 3 h at 30 °C together with BDNF #2 antibody coupled to HRP. Plates were washed three times with TBST. SuperSignal ELISA Femto Substrate (Life Technologies), diluted 50% in H_2O, was used as the substrate. With these modifications to the assay, we improved its sensitivity to detect 1 pg of BDNF per well. In addition, using a range of standards with different amounts of

recombinant BDNF (1–1024 pg/well), we generated standard curves for each experiment performed, which allowed us to precisely quantify the BDNF present in striatal tissue. The following antibodies were used [101]: mouse BDNF monoclonal (Developmental Studies Hybridoma Bank) for ELISA, BDNF #1 at 1 μg/well for plate coating, and HRP-labeled BDNF #2 at 12 ng/well.

Dendritic Spine Dying and Confocal Analysis Neurons were labeled using the Helios Gene Gun System (Bio-Rad) as previously described [102]. Briefly, a suspension containing 3 mg of DiI (Molecular Probes, Invitrogen) dissolved in 100 μl of methylene chloride (Sigma) and mixed with 50 mg of tungsten particles (1.7 mm diameter, Bio-Rad) was spread on a glass slide and air-dried. The mixture was resuspended in 3.5 ml distilled water and sonicated. Subsequently, the mixture was drawn into Tefzel tubing (Bio-Rad) and then removed to let tube dry during 5 min under a nitrogen flow gas. Then, the tube was cut into 13 mm pieces to be used as bio gun's cartridges. Dye-coated particles were delivered in the striatum using the following protocol. Shooting was performed over 150 μm coronal sections at 80 psi through a membrane filter of 3 μm pore size and 8×10 pores/cm^2 (Millipore). Sections were stored at room temperature in PBS for 3 h protected from light, then incubated with DAPI, and finally mounted with Mowiol to be analyzed. DiI-labeled medium spiny neurons of the dorsal striatum were imaged using a Leica Confocal SP5 with a × 63 oil-immersion objective. Conditions such as pinhole size (1 AU) and frame averaging (4 frames/z-step) were held constant throughout the study. Confocal z-stacks were taken with a digital zoom of 5, a z-step of 0.2 μm, and a resolution of 1024 × 1024 pixel, yielding an image with pixel dimensions of 49.25 × 49.25 μm. Z-stacks were deconvolved using the Acoloma plugins from ImageJ to improve voxel resolution and reduce optical aberration along the *z*-axis. Segments from MSN dendrites were selected for the analysis of spine density according the following criteria: (1) segments with no overlap with other branches that would obscure visualization of spines and (2) segments either "parallel to" or "at acute angles" relative to the coronal surface of the section to avoid unambiguous identification of spines. Only spines arising from the lateral surfaces of the dendrites were included in the study, ignoring spines located on the top or bottom of the dendrite surface. Given that spine density increases as a function of the distance from the soma, reaching a plateau 45 μm away from the soma, we selected dendritic segments of basal dendrites 45 μm away from the cell body.

Immunohistochemistry For immunohistochemical analysis, mice were deeply anesthetized and immediately perfused transcardially with saline followed by 4% paraformaldehyde/phosphate buffer. The brains were removed and postfixed overnight in the same solution, cryoprotected by immersion in 30% sucrose, and then frozen in dry ice-cooled methylbutane. Serial coronal cryostat sections (30 μm) through the whole brain were collected in PBS as free-floating sections.

For EM48 immunohistochemistry, sections were first incubated for 30 min in a 0.01 M sodium citrate buffer (pH 6) preheated to and maintained at 80 °C in a water bath (just for KI and KI:p75$^{+/-}$ animals). Next, endogenous peroxidases were blocked for 45 min in PBS containing 3% H_2O_2. Non-specific protein interactions were blocked with 3% normal horse serum. Tissue was incubated overnight at 4 °C with the primary antibody anti-EM48 (1:500, Millipore). Sections were washed three times in PBS and incubated with a biotinylated anti-mouse antibody (1:200; Pierce) at room temperature for 2 h. The immunohistochemical reaction was developed using the ABC kit (Pierce) and made visible with diaminobenzidine. No signal was detected in controls in which the primary antibodies had been omitted. Automated quantification of the number of nuclear huntingtin aggregates and the number and intensity of EM48-stained nuclei within the striatum were performed using CellProfiler v2.8 software. Three coronal striatal sections per animal spaced 240 μm apart were chosen for the analysis. Bright field images from the 100% of the striatum were acquired at × 40 magnification with a BX51 Olympus microscope with the cast system software (Olympus Danmark A/S). The CellProfiler pipeline file containing the specific parameters of the automated quantification is available upon request. In particular, for KI and KI:p75$^{+/-}$ striatal sections, diffuse EM48 immunostaining was quantified as a "staining index" that captures both the nuclear staining intensity and the number of immunostained nuclei, as described previously [103, 104].

For cleaved caspase-3 immunohistochemistry, sections were rinsed two times in PBS, treated with 50 mM NH4Cl for 30 min, rinsed three more times in PBS, and permeabilized and blocked in PBS containing 0.3% Triton X-100 and 10% normal horse serum (Pierce Biotechnology) for 90 min at room temperature. Sections were then washed in PBS and incubated overnight at 4 °C with the primary antibody anti-cleaved caspase-3 (1:250, Cell Signaling). Slices were washed three times and then incubated 2 h shaking at room temperature with the secondary antibody anti-rabbit Cy3 555 (1:100, Jackson Immuno Research). Nuclei were stained with Hoechst 33258 (1:10,000, Molecular Probes, Life Technologies) for 10 min. No signal was detected in controls in which the primary antibodies had been omitted. As positive controls, sections were obtained from animals which had undergone physical lesion in the corticostriatal region causing cell apoptosis. Images were acquired with a BX60 epifluorescence microscope (Olympus) with an Orca-ER cooled CCD camera (Hamamatsu).

Nissl Staining Nissl staining was performed in floating sections (30 μm, three sections/mouse) after incubation with cresyl violet solution (0.1 g/L) for 45 min. Images were acquired at × 4 with a BX51 Olympus microscope, and thickness of motor cortex (M1) was measured using ImageJ.

Statistical Analysis All data are expressed as mean ± SEM. Statistical analysis was performed by using the unpaired Student's *t* test (95% confidence), one-way ANOVA, two-way ANOVA, and the appropriate posthoc tests as indicated in the figure legends. Values of $P < 0.05$ were considered as statistically significant.

Acknowledgements We are very grateful to Ana Lopez and Maria Teresa Muñoz for technical assistance, Dr. Teresa Rodrigo and the staff of the animal care facility (Facultat de Psicologia Universitat de Barcelona), and Dr. Maria Calvo, Anna Bosch, and Elisenda Coll from the Advanced Optical Microscopy Unit from Scientific and Technological Centers from University of Barcelona for their support and advice with confocal technique.

Authors' Contributions N.S contributed to the design and carried out the biochemical and immunohistochemical studies, analyzed, interpreted data, and participated in the manuscript draft. A.M contributed to the design and carried out the pharmacological studies in R6/1 mice, analyzed, and interpreted data. S.L.B contributed to the design and carried out the ELISA studies, as well as analyzed and interpreted data. G.G.D.B contributed to the design and carried out the biochemical studies in the R6/1 mice, as well as analyzed and interpreted data. A.G participated in behavioral studies in the KI:$p75^{+/-}$ mice, as well as analyzed and interpreted data. E.A.P carried out immunohistochemistry. J.C.A revised and commented the manuscript. J.A revised and commented the manuscript. S.G contributed to data interpretation, to experimental design, and to the manuscript draft. V.B conceived the study, contributed to the design and carried out behavioral and dendritic spine studies, analyzed and interpreted data, wrote the manuscript, and edited the document. All authors read and approved the final manuscript.

Funding This work was supported by the Ministerio de Ciencia e Innovación (SAF-2014-57160R to J.A and SAF2015-67474-R; MINECO/FEDER to S.G), the Centro de Investigaciones Biomédicas en Red sobre Enfermedades Neurodegenerativas (CIBERNED), and the Cure Huntington's Disease Initiative (CHDI A-3468).

Compliance with Ethical Standards

Experimental procedures were approved by the Local Ethical Committee of the University of Barcelona (99/01) and the Generalitat de Catalunya (00/1094), following European (2010/63/UE) and Spanish (RD 1201/2005) regulations for the care and use of laboratory animals.

Conflict of Interest The authors declare that they have no conflict of interest.

Abbreviations A2AR, adenosine receptor type 2A; BDNF, brain-derived neurotrophic factor; DARPP32, dopamine- and cAMP-regulated phosphoprotein, Mr 32 kDa; HD, Huntington's disease; Htt, huntingtin; JNK, c-Jun kinase; KI, knock-in; PLCγ, phospholipase C gamma; PDE10A, phosphodiesterase 10A; mHtt, mutant huntingtin; MSN, medium spiny neuron; WT, wild type

References

1. Walker FO (2007) Huntington's disease. Lancet 369:218–228
2. The Huntington's Disease Collaborative Research Group (1993) A novel gene containing a trinucleotide repeat that is expanded and unstable on Huntington's disease chromosomes. Cell 72:971–983
3. Vonsattel JP, Myers RH, Stevens TJ, Ferrante RJ, Bird ED, Richardson EPJ (1985) Neuropathological classification of Huntington's disease. J Neuropathol Exp Neurol 44:559–577
4. DiFiglia M, Sapp E, Chase KO, Davies SW, Bates GP, Vonsattel JP, Aronin N (1997) Aggregation of huntingtin in neuronal intranuclear inclusions and dystrophic neurites in brain. Science 277:1990–1993
5. Ivkovic S, Ehrlich ME (1999) Expression of the striatal DARPP-32/ARPP-21 phenotype in GABAergic neurons requires neurotrophins in vivo and in vitro. J Neurosci 19:5409–5419
6. Baydyuk M, Russell T, Liao G-Y, Zang K, An JJ, Reichardt LF, Xu B (2011) TrkB receptor controls striatal formation by regulating the number of newborn striatal neurons. Proc Natl Acad Sci U S A 108:1669–1674
7. Zuccato C, Ciammola A, Rigamonti D, Leavitt BR, Goffredo D, Conti L, MacDonald ME, Friedlander RM et al (2001) Loss of huntingtin-mediated BDNF gene transcription in Huntington's disease. Science 293:493–498
8. Gauthier LR, Charrin BC, Borrell-Pages M, Dompierre JP, Rangone H, Cordelieres FP, De Mey J, MacDonald ME et al (2004) Huntingtin controls neurotrophic support and survival of neurons by enhancing BDNF vesicular transport along microtubules. Cell 118:127–138
9. Zuccato C, Cattaneo E (2009) Brain-derived neurotrophic factor in neurodegenerative diseases. Nat Rev Neurol 5:311–322
10. Ma Q, Yang J, Li T, Milner TA, Hempstead BL (2015) Selective reduction of striatal mature BDNF without induction of proBDNF in the zQ175 mouse model of Huntington's disease. Neurobiol Dis 82:466–477
11. Gharami K, Xie Y, An JJ, Tonegawa S, Xu B (2008) Brain-derived neurotrophic factor over-expression in the forebrain ameliorates Huntington's disease phenotypes in mice. J Neurochem 105:369–379
12. Giralt A, Friedman HC, Caneda-Ferron B, Urban N, Moreno E, Rubio N, Blanco J, Peterson A et al (2010) BDNF regulation under GFAP promoter provides engineered astrocytes as a new approach for long-term protection in Huntington's disease. Gene Ther 17:1294–1308
13. Xie Y, Hayden MR, Xu B (2010) BDNF overexpression in the forebrain rescues Huntington's disease phenotypes in YAC128 mice. J Neurosci 30:14708–14718
14. Simmons DA, Belichenko NP, Yang T, Condon C, Monbureau M, Shamloo M, Jing D, Massa SM et al (2013) A small molecule TrkB ligand reduces motor impairment and neuropathology in R6/2 and BACHD mouse models of Huntington's disease. J Neurosci 33:18712–18727
15. Gines S, Bosch M, Marco S, Gavalda N, Diaz-Hernandez M, Lucas JJ, Canals JM, Alberch J (2006) Reduced expression of the TrkB receptor in Huntington's disease mouse models and in human brain. Eur J Neurosci 23:649–658
16. Zuccato C, Marullo M, Conforti P, MacDonald ME, Tartari M, Cattaneo E (2008) Systematic assessment of BDNF and its receptor levels in human cortices affected by Huntington's disease. Brain Pathol 18:225–238
17. Gines S, Paoletti P, Alberch J (2010) Impaired TrkB-mediated ERK1/2 activation in Huntington disease knock-in striatal cells

involves reduced p52/p46 Shc expression. J Biol Chem 285: 21537–21548
18. Liot G, Zala D, Pla P, Mottet G, Piel M, Saudou F (2013) Mutant huntingtin alters retrograde transport of TrkB receptors in striatal dendrites. J Neurosci 33:6298–6309
19. Brito V, Puigdellivol M, Giralt A, del Toro D, Alberch J, Gines S (2013) Imbalance of p75(NTR)/TrkB protein expression in Huntington's disease: implication for neuroprotective therapies. Cell Death Dis 4:e595
20. Plotkin JL, Day M, Peterson JD, Xie Z, Kress GJ, Rafalovich I, Kondapalli J, Gertler TS et al (2014) Impaired TrkB receptor signaling underlies corticostriatal dysfunction in Huntington's disease. Neuron 83:178–188
21. Nguyen KQ, Rymar VV, Sadikot AF (2016) Impaired TrkB signaling underlies reduced BDNF-mediated trophic support of striatal neurons in the R6/2 mouse model of Huntington's disease. Front Cell Neurosci 10:37
22. Baker SJ, Reddy EP (1996) Transducers of life and death: TNF receptor superfamily and associated proteins. Oncogene 12:1–9
23. Yamashita T, Tucker KL, Barde YA (1999) Neurotrophin binding to the p75 receptor modulates rho activity and axonal outgrowth. Neuron 24:585–593
24. Roux PP, Barker PA (2002) Neurotrophin signaling through the p75 neurotrophin receptor. Prog Neurobiol 67:203–233
25. Yamashita T, Tohyama M (2003) The p75 receptor acts as a displacement factor that releases rho from rho-GDI. Nat Neurosci 6: 461–467
26. Yoon SO, Casaccia-Bonnefil P, Carter B, Chao MV (1998) Competitive signaling between TrkA and p75 nerve growth factor receptors determines cell survival. J Neurosci 18:3273–3281
27. Fortress AM, Buhusi M, Helke KL, Granholm A-CE (2011) Cholinergic degeneration and alterations in the TrkA and p75NTR balance as a result of pro-NGF injection into aged rats. J Aging Res 2011:460543
28. Brito V, Giralt A, Enriquez-Barreto L, Puigdellivol M, Suelves N, Zamora-Moratalla A, Ballesteros JJ, Martin ED et al (2014) Neurotrophin receptor p75(NTR) mediates Huntington's disease-associated synaptic and memory dysfunction. J Clin Invest 124: 4411–4428
29. Miguez A, Garcia-Diaz Barriga G, Brito V, Straccia M, Giralt A, Gines S, Canals JM, Alberch J (2015) Fingolimod (FTY720) enhances hippocampal synaptic plasticity and memory in Huntington's disease by preventing p75NTR up-regulation and astrocyte-mediated inflammation. Hum Mol Genet 24:4958–4970
30. Simmons DA, Belichenko NP, Ford EC, Semaan S, Monbureau M, Aiyaswamy S, Holman CM, Condon C et al (2016) A small molecule p75NTR ligand normalizes signalling and reduces Huntington's disease phenotypes in R6/2 and BACHD mice. Hum Mol Genet 25:4920–4938
31. Puigdellivol M, Cherubini M, Brito V, Giralt A, Suelves N, Ballesteros J, Zamora-Moratalla A, Martin ED et al (2015) A role for Kalirin-7 in corticostriatal synaptic dysfunction in Huntington's disease. Hum Mol Genet 24:7265–7285
32. Bibb JA, Yan Z, Svenningsson P, Snyder GL, Pieribone VA, Horiuchi A, Nairn AC, Messer A et al (2000) Severe deficiencies in dopamine signaling in presymptomatic Huntington's disease mice. Proc Natl Acad Sci U S A 97:6809–6814
33. Niccolini F, Haider S, Reis Marques T, Muhlert N, Tziortzi AC, Searle GE, Natesan S, Piccini P et al (2015) Altered PDE10A expression detectable early before symptomatic onset in Huntington's disease. Brain 138:3016–3029
34. Popoli P, Blum D, Domenici MR, Burnouf S, Chern Y (2008) A critical evaluation of adenosine A2A receptors as potentially "druggable" targets in Huntington's disease. Curr Pharm Des 14: 1500–1511
35. Spires TL, Grote HE, Garry S, Cordery PM, Van Dellen A, Blakemore C, Hannan AJ (2004) Dendritic spine pathology and deficits in experience-dependent dendritic plasticity in R6/1 Huntington's disease transgenic mice. Eur J Neurosci 19:2799–2807
36. Murmu RP, Li W, Holtmaat A, Li J-Y (2013) Dendritic spine instability leads to progressive neocortical spine loss in a mouse model of Huntington's disease. J Neurosci 33:12997–13009
37. Zagrebelsky M, Holz A, Dechant G, Barde Y-A, Bonhoeffer T, Korte M (2005) The p75 neurotrophin receptor negatively modulates dendrite complexity and spine density in hippocampal neurons. J Neurosci 25:9989–9999
38. Yang J, Siao C-J, Nagappan G, Marinic T, Jing D, McGrath K, Chen Z-Y, Mark W et al (2009) Neuronal release of proBDNF. Nat Neurosci 12:113–115
39. Chapman TR, Barrientos RM, Ahrendsen JT, Hoover JM, Maier SF, Patterson SL (2012) Aging and infection reduce expression of specific brain-derived neurotrophic factor mRNAs in hippocampus. Neurobiol Aging 33:832.e1–832.14
40. Calabrese F, Guidotti G, Racagni G, Riva MA (2013) Reduced neuroplasticity in aged rats: a role for the neurotrophin brain-derived neurotrophic factor. Neurobiol Aging 34:2768–2776
41. Zuccato C, Liber D, Ramos C, Tarditi A, Rigamonti D, Tartari M, Valenza M, Cattaneo E (2005) Progressive loss of BDNF in a mouse model of Huntington's disease and rescue by BDNF delivery. Pharmacol Res 52:133–139
42. Altar CA, Cai N, Bliven T, Juhasz M, Conner JM, Acheson AL, Lindsay RM, Wiegand SJ (1997) Anterograde transport of brain-derived neurotrophic factor and its role in the brain. Nature 389: 856–860
43. Minichiello L, Calella AM, Medina DL, Bonhoeffer T, Klein R, Korte M (2002) Mechanism of TrkB-mediated hippocampal long-term potentiation. Neuron 36:121–137
44. Huang EJ, Reichardt LF (2003) Trk receptors: roles in neuronal signal transduction. Annu Rev Biochem 72:609–642
45. Bowles KR, Jones L (2014) Kinase signalling in Huntington's disease. J Huntingtons Dis 3:89–123
46. Saavedra A, Garcia-Martinez JM, Xifro X, Giralt A, Torres-Peraza JF, Canals JM, Diaz-Hernandez M, Lucas JJ et al (2010) PH domain leucine-rich repeat protein phosphatase 1 contributes to maintain the activation of the PI3K/Akt pro-survival pathway in Huntington's disease striatum. Cell Death Differ 17:324–335
47. Gines S, Ivanova E, Seong I-S, Saura CA, MacDonald ME (2003) Enhanced Akt signaling is an early pro-survival response that reflects N-methyl-D-aspartate receptor activation in Huntington's disease knock-in striatal cells. J Biol Chem 278:50514–50522
48. Apostol BL, Simmons DA, Zuccato C, Illes K, Pallos J, Casale M, Conforti P, Ramos C et al (2008) CEP-1347 reduces mutant huntingtin-associated neurotoxicity and restores BDNF levels in R6/2 mice. Mol Cell Neurosci 39:8–20
49. Perrin V, Dufour N, Raoul C, Hassig R, Brouillet E, Aebischer P, Luthi-Carter R, Deglon N (2009) Implication of the JNK pathway in a rat model of Huntington's disease. Exp Neurol 215:191–200
50. Taylor DM, Moser R, Regulier E, Breuillaud L, Dixon M, Beesen AA, Elliston L, de Silva Santos M, F et al (2013) MAP kinase phosphatase 1 (MKP-1/DUSP1) is neuroprotective in Huntington's disease via additive effects of JNK and p38 inhibition. J Neurosci 33:2313–2325
51. Bragg RM, Coffey SR, Weston RM, Ament SA, Cantle JP, Minnig S, Funk CC, Shuttleworth DD et al (2017) Motivational, proteostatic and transcriptional deficits precede synapse loss,

gliosis and neurodegeneration in the B6.HttQ111/+ model of Huntington's disease. Sci Rep 7:41570
52. Anglada-Huguet M, Xifro X, Giralt A, Zamora-Moratalla A, Martin ED, Alberch J (2014) Prostaglandin E2 EP1 receptor antagonist improves motor deficits and rescues memory decline in R6/1 mouse model of Huntington's disease. Mol Neurobiol 49: 784–795
53. Garcia-Diaz Barriga G, Giralt A, Anglada-Huguet M, Gaja-Capdevila N, Orlandi JG, Soriano J, Canals J-M, Alberch J (2017) 7,8-Dihydroxyflavone ameliorates cognitive and motor deficits in a Huntington's disease mouse model through specific activation of the PLCgamma1 pathway. Hum Mol Genet 26:3144–3160
54. Canals JM, Pineda JR, Torres-Peraza JF, Bosch M, Martin-Ibanez R, Munoz MT, Mengod G, Ernfors P et al (2004) Brain-derived neurotrophic factor regulates the onset and severity of motor dysfunction associated with enkephalinergic neuronal degeneration in Huntington's disease. J Neurosci 24:7727–7739
55. Nishi A, Kuroiwa M, Miller DB, O'Callaghan JP, Bateup HS, Shuto T, Sotogaku N, Fukuda T et al (2008) Distinct roles of PDE4 and PDE10A in the regulation of cAMP/PKA signaling in the striatum. J Neurosci 28:10460–10471
56. Girault J-A (2012) Integrating neurotransmission in striatal medium spiny neurons. Adv Exp Med Biol 970:407–429
57. Cui G, Jun SB, Jin X, Pham MD, Vogel SS, Lovinger DM, Costa RM (2013) Concurrent activation of striatal direct and indirect pathways during action initiation. Nature 494:238–242
58. Diogenes MJ, Fernandes CC, Sebastiao AM, Ribeiro JA (2004) Activation of adenosine A2A receptor facilitates brain-derived neurotrophic factor modulation of synaptic transmission in hippocampal slices. J Neurosci 24:2905–2913
59. Fontinha BM, Diogenes MJ, Ribeiro JA, Sebastiao AM (2008) Enhancement of long-term potentiation by brain-derived neurotrophic factor requires adenosine A2A receptor activation by endogenous adenosine. Neuropharmacology 54:924–933
60. Sebastiao AM, Assaife-Lopes N, Diogenes MJ, Vaz SH, Ribeiro JA (2011) Modulation of brain-derived neurotrophic factor (BDNF) actions in the nervous system by adenosine A(2A) receptors and the role of lipid rafts. Biochim Biophys Acta 1808:1340–1349
61. Svenningsson P, Nishi A, Fisone G, Girault J-A, Nairn AC, Greengard P (2004) DARPP-32: an integrator of neurotransmission. Annu Rev Pharmacol Toxicol 44:269–296
62. Fernandez E, Schiappa R, Girault J-A, Le Novere N (2006) DARPP-32 is a robust integrator of dopamine and glutamate signals. PLoS Comput Biol 2:e176
63. Yger M, Girault J-A (2011) DARPP-32, Jack of all trades… Master of which? Front Behav Neurosci 5:56
64. Engmann O, Giralt A, Gervasi N, Marion-Poll L, Gasmi L, Filhol O, Picciotto MR, Gilligan D et al (2015) DARPP-32 interaction with adducin may mediate rapid environmental effects on striatal neurons. Nat Commun 6:10099
65. Smith GA, Rocha EM, McLean JR, Hayes MA, Izen SC, Isacson O, Hallett PJ (2014) Progressive axonal transport and synaptic protein changes correlate with behavioral and neuropathological abnormalities in the heterozygous Q175 KI mouse model of Huntington's disease. Hum Mol Genet 23:4510–4527
66. Spires TL, Grote HE, Varshney NK, Cordery PM, van Dellen A, Blakemore C, Hannan AJ (2004) Environmental enrichment rescues protein deficits in a mouse model of Huntington's disease, indicating a possible disease mechanism. J Neurosci 24:2270–2276
67. Zala D, Colin E, Rangone H, Liot G, Humbert S, Saudou F (2008) Phosphorylation of mutant huntingtin at S421 restores anterograde and retrograde transport in neurons. Hum Mol Genet 17:3837–3846
68. Kraemer BR, Snow JP, Vollbrecht P, Pathak A, Valentine WM, Deutch AY, Carter BD (2014) A role for the p75 neurotrophin receptor in axonal degeneration and apoptosis induced by oxidative stress. J Biol Chem 289:21205–21216
69. Gatto RG, Chu Y, Ye AQ, Price SD, Tavassoli E, Buenaventura A, Brady ST, Magin RL et al (2015) Analysis of YFP(J16)-R6/2 reporter mice and postmortem brains reveals early pathology and increased vulnerability of callosal axons in Huntington's disease. Hum Mol Genet England 24:5285–5298. https://doi.org/10.1093/hmg/ddv248
70. Li J-Y, Conforti L (2013) Axonopathy in Huntington's disease. Exp Neurol 246:62–71
71. Lee FS, Rajagopal R, Chao MV (2002) Distinctive features of Trk neurotrophin receptor transactivation by G protein-coupled receptors. Cytokine Growth Factor Rev 13:11–17
72. Rajagopal R, Chen Z-Y, Lee FS, Chao MV (2004) Transactivation of Trk neurotrophin receptors by G-protein-coupled receptor ligands occurs on intracellular membranes. J Neurosci 24:6650–6658
73. Berghuis P, Dobszay MB, Wang X, Spano S, Ledda F, Sousa KM, Schulte G, Ernfors P et al (2005) Endocannabinoids regulate interneuron migration and morphogenesis by transactivating the TrkB receptor. Proc Natl Acad Sci U S A 102:19115–19120
74. Lewis MA, Hunihan L, Franco D, Robertson B, Palmer J, Laurent DRS, Balasubramanian BN, Li Y et al (2006) Identification and characterization of compounds that potentiate NT-3-mediated Trk receptor activity. Mol Pharmacol 69:1396–1404
75. Vesa J, Kruttgen A, Shooter EM (2000) p75 reduces TrkB tyrosine autophosphorylation in response to brain-derived neurotrophic factor and neurotrophin 4/5. J Biol Chem 275:24414–24420
76. Sakuragi S, Tominaga-Yoshino K, Ogura A (2013) Involvement of TrkB- and p75(NTR)-signaling pathways in two contrasting forms of long-lasting synaptic plasticity. Sci Rep 3:3185
77. Bibel M, Hoppe E, Barde YA (1999) Biochemical and functional interactions between the neurotrophin receptors trk and p75NTR. EMBO J 18:616–622
78. Jang H-J, Yang YR, Kim JK, Choi JH, Seo Y-K, Lee YH, Lee JE, Ryu SH et al (2013) Phospholipase C-gamma1 involved in brain disorders. Adv Biol Regul 53:51–62
79. Stroppolo A, Guinea B, Tian C, Sommer J, Ehrlich ME (2001) Role of phosphatidylinositide 3-kinase in brain-derived neurotrophic factor-induced DARPP-32 expression in medium size spiny neurons in vitro. J Neurochem 79:1027–1032
80. Chiang M-C, Lee Y-C, Huang C-L, Chern Y (2005) cAMP-response element-binding protein contributes to suppression of the A2A adenosine receptor promoter by mutant huntingtin with expanded polyglutamine residues. J Biol Chem 280:14331–14340
81. Horne EA, Dell'Acqua ML (2007) Phospholipase C is required for changes in postsynaptic structure and function associated with NMDA receptor-dependent long-term depression. J Neurosci 27: 3523–3534
82. Zhou L, Martinez SJ, Haber M, Jones EV, Bouvier D, Doucet G, Corera AT, Fon EA et al (2007) EphA4 signaling regulates phospholipase Cgamma1 activation, cofilin membrane association, and dendritic spine morphology. J Neurosci 27:5127–5138
83. Kim K, Yang J, Kim E (2010) Diacylglycerol kinases in the regulation of dendritic spines. J Neurochem 112:577–587
84. Meriin AB, Mabuchi K, Gabai VL, Yaglom JA, Kazantsev A, Sherman MY (2001) Intracellular aggregation of polypeptides with expanded polyglutamine domain is stimulated by stress-activated kinase MEKK1. J Cell Biol 153:851–864

85. Cowan KJ, Diamond MI, Welch WJ (2003) Polyglutamine protein aggregation and toxicity are linked to the cellular stress response. Hum Mol Genet 12:1377–1391
86. Scappini E, Koh T-W, Martin NP, O'Bryan JP (2007) Intersectin enhances huntingtin aggregation and neurodegeneration through activation of c-Jun-NH2-terminal kinase. Hum Mol Genet 16: 1862–1871
87. Morfini GA, You Y-M, Pollema SL, Kaminska A, Liu K, Yoshioka K, Bjorkblom B, Coffey ET, Bagnato C, Han D, Huang C-F, Banker G, Pigino G, et al. Pathogenic huntingtin inhibits fast axonal transport by activating JNK3 and phosphorylating kinesin. Nat Neurosci. United States; 2009; 12: 864–71. doi: https://doi.org/10.1038/nn.2346.
88. Bauer PO, Wong HK, Oyama F, Goswami A, Okuno M, Kino Y, Miyazaki H, Nukina N (2009) Inhibition of rho kinases enhances the degradation of mutant huntingtin. J Biol Chem 284:13153–13164
89. Bauer PO, Nukina N (2009) Enhanced degradation of mutant huntingtin by rho kinase inhibition is mediated through activation of proteasome and macroautophagy. Autophagy 5:747–748
90. Li M, Huang Y, Ma AAK, Lin E, Diamond MI (2009) Y-27632 improves rotarod performance and reduces huntingtin levels in R6/2 mice. Neurobiol Dis 36:413–420
91. Hensel N, Rademacher S, Claus P (2015) Chatting with the neighbors: crosstalk between rho-kinase (ROCK) and other signaling pathways for treatment of neurological disorders. Front Neurosci 9:198
92. Deogracias R, Yazdani M, Dekkers MPJ, Guy J, Ionescu MCS, Vogt KE, Barde Y-A (2012) Fingolimod, a sphingosine-1 phosphate receptor modulator, increases BDNF levels and improves symptoms of a mouse model of Rett syndrome. Proc Natl Acad Sci U S A 109:14230–14235
93. Di Pardo A, Amico E, Favellato M, Castrataro R, Fucile S, Squitieri F, Maglione V (2014) FTY720 (fingolimod) is a neuroprotective and disease-modifying agent in cellular and mouse models of Huntington disease. Hum Mol Genet 23:2251–2265
94. Pang TYC, Stam NC, Nithianantharajah J, Howard ML, Hannan AJ (2006) Differential effects of voluntary physical exercise on behavioral and brain-derived neurotrophic factor expression deficits in Huntington's disease transgenic mice. Neuroscience 141:569–584
95. Hait NC, Wise LE, Allegood JC, O'Brien M, Avni D, Reeves TM, Knapp PE, Lu J et al (2014) Active, phosphorylated fingolimod inhibits histone deacetylases and facilitates fear extinction memory. Nat Neurosci 17:971–980
96. Cragnolini AB, Friedman WJ (2008) The function of p75NTR in glia. Trends Neurosci 31:99–104
97. Cragnolini AB, Huang Y, Gokina P, Friedman WJ (2009) Nerve growth factor attenuates proliferation of astrocytes via the p75 neurotrophin receptor. Glia 57:1386–1392
98. Han I, You Y, Kordower JH, Brady ST, Morfini GA (2010) Differential vulnerability of neurons in Huntington's disease: the role of cell type-specific features. J Neurochem England 113: 1073–1091. https://doi.org/10.1111/j.1471-4159.2010.06672.x
99. Wheeler VC, Auerbach W, White JK, Srinidhi J, Auerbach A, Ryan A, Duyao MP, Vrbanac V et al (1999) Length-dependent gametic CAG repeat instability in the Huntington's disease knock-in mouse. Hum Mol Genet 8:115–122
100. Mangiarini L, Sathasivam K, Seller M, Cozens B, Harper A, Hetherington C, Lawton M, Trottier Y et al (1996) Exon 1 of the HD gene with an expanded CAG repeat is sufficient to cause a progressive neurological phenotype in transgenic mice. Cell 87: 493–506
101. Kolbeck R, Bartke I, Eberle W, Barde YA (1999) Brain-derived neurotrophic factor levels in the nervous system of wild-type and neurotrophin gene mutant mice. J Neurochem 72:1930–1938
102. Grutzendler J, Tsai J, Gan W-B (2003) Rapid labeling of neuronal populations by ballistic delivery of fluorescent dyes. Methods 30: 79–85
103. Lloret A, Dragileva E, Teed A, Espinola J, Fossale E, Gillis T, Lopez E, Myers RH et al (2006) Genetic background modifies nuclear mutant huntingtin accumulation and HD CAG repeat instability in Huntington's disease knock-in mice. Hum Mol Genet 15:2015–2024
104. Pinto RM, Dragileva E, Kirby A, Lloret A, Lopez E, St Claire J, Panigrahi GB, Hou C et al (2013) Mismatch repair genes Mlh1 and Mlh3 modify CAG instability in Huntington's disease mice: genome-wide and candidate approaches. PLoS Genet 9:e1003930